AD-A171 724 AN INVESTIGATION INTO THE EFFECTS OF FUEL ADDITIVES AND 1/1
FUEL COMPOSITION O (U) NAVAL POSTGRADUATE SCHOOL
MONTEREY CA J C HUA JUN 86

UNCLASSIFIED F/G 21/2 NL

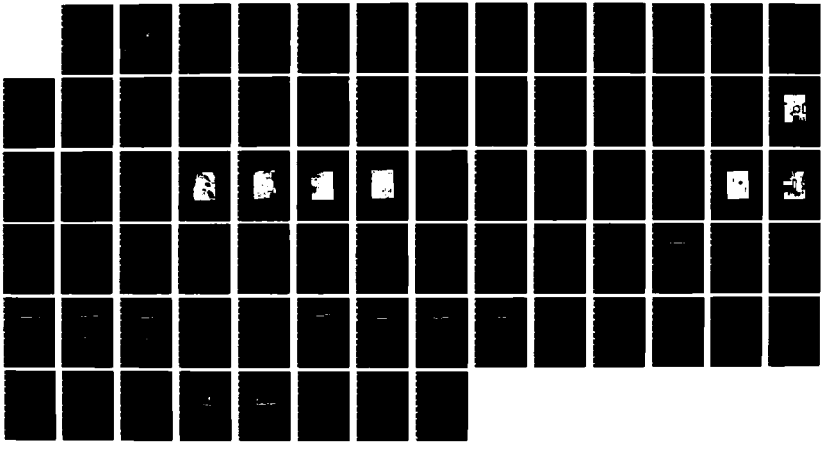

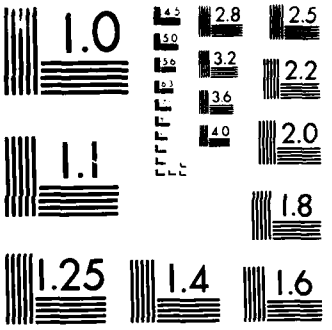
1.0
1.1
1.25
1.4
1.6
1.8
2.0
2.2
2.5
2.8
3.2
3.6
4.0
4.5
5.0
5.6
6.3
7.1
8.0
9.0
10.0

NAVAL POSTGRADUATE SCHOOL

Monterey, California

THESIS

AN INVESTIGATION INTO THE EFFECTS OF FUEL ADDITIVES AND FUEL COMPOSITION ON SOOT PARTICLE SIZE IN A T63 GAS TURBINE COMBUSTOR USING LIGHT TRANSMITTANCE AND SCATTERING TECHNIQUES

by

Jway Ching Hua

June 1986

Thesis Advisor: David W. Netzer

Approved for public release; distribuion is unlimited

AD-A171724

SECURITY CLASSIFICATION OF THIS PAGE

REPORT DOCUMENTATION PAGE

1a REPORT SECURITY CLASSIFICATION: Unclassified	1b. RESTRICTIVE MARKINGS
2a SECURITY CLASSIFICATION AUTHORITY	3 DISTRIBUTION/AVAILABILITY OF REPORT: Approved for public release; distribution is unlimited
2b DECLASSIFICATION/DOWNGRADING SCHEDULE	
4 PERFORMING ORGANIZATION REPORT NUMBER(S)	5 MONITORING ORGANIZATION REPORT NUMBER(S)
6a NAME OF PERFORMING ORGANIZATION: Naval Postgraduate School; 6b OFFICE SYMBOL (If applicable): Code 67	7a. NAME OF MONITORING ORGANIZATION: Naval Postgraduate School
6c ADDRESS (City, State, and ZIP Code): Monterey, California 93943-5100	7b. ADDRESS (City, State, and ZIP Code): Monterey, California 93943-5100
8a NAME OF FUNDING/SPONSORING ORGANIZATION: Naval Air Propulsion Center; 8b. OFFICE SYMBOL (If applicable)	9. PROCUREMENT INSTRUMENT IDENTIFICATION NUMBER
8c ADDRESS (City, State, and ZIP Code): Trenton, N.J. 08628-0176	10 SOURCE OF FUNDING NUMBERS: PROGRAM ELEMENT NO; PROJECT NO N62376 86WR00013; TASK NO; WORK UNIT ACCESSION NO

11 TITLE (Include Security Classification) AN INVESTIGATION INTO THE EFFECTS OF FUEL ADDITIVES AND FUEL COMPOSITION ON SOOT PARTICLE SIZE IN A T63 GAS TURBINE COMBUSTOR USING LIGHT TRANSMITTANCE AND SCATTERING TECHNIQUES

12 PERSONAL AUTHOR(S) Jway Ching Hua

13a TYPE OF REPORT	13b TIME COVERED FROM ____ TO ____	14 DATE OF REPORT (Year, Month, Day)	15 PAGE COUNT
Master's Thesis		1986 June	75

16 SUPPLEMENTARY NOTATION

17 COSATI CODES			18 SUBJECT TERMS (Continue on reverse if necessary and identify by block number)
FIELD	GROUP	SUB-GROUP	Soot Particle Size, Light Transmittance, Scattering

19 ABSTRACT (Continue on reverse if necessary and identify by block number) An experimental investigation was conducted to examine the effects of fuel-air ratios, fuel composition and smoke-suppressant fuel additives on the sooting characteristics of a T-63 combustor. Multiple wavelength light transmission and two-angle light scattering measurements were used to measure the mean soot diameter. Ferrocene, 12% Cerium Hex-Cem and USLAD 2055 were found effective in reducting exhaust gas opacity. Initial results were conflicting on the cause for the reduced opacity.

20 DISTRIBUTION/AVAILABILITY OF ABSTRACT: ☒ UNCLASSIFIED/UNLIMITED ☐ SAME AS RPT ☐ DTIC USERS	21. ABSTRACT SECURITY CLASSIFICATION: Unclassified
22a NAME OF RESPONSIBLE INDIVIDUAL: David W. Netzer	22b TELEPHONE (Include Area Code): (408) 646-2980; 22c. OFFICE SYMBOL: 67Nt

DD FORM 1473, 84 MAR 83 APR edition may be used until exhausted. All other editions are obsolete.

SECURITY CLASSIFICATION OF THIS PAGE

Approved for public release; distribution is unlimited.

An Investigation Into The Effects of Fuel Additives and Fuel Composition on Soot Particle Size in a T63 Gas Turbine Combustor Using Light Transmittance and Scattering Techniques

by

Jway Ching Hua
Captain, Republic of Singapore Navy
dipl., Singapore Polytechnic, 1974

Submitted in partial fulfillment of the requirements for the degree of

MASTER OF SCIENCE IN ENGINEERING SCIENCE

from the

NAVAL POSTGRADUATE SCHOOL
June 1986

Author: Jway Ching Hua

Approved by: David W. Netzer, Thesis Advisor

M. F. Platzer, Chairman,
Department of Aeronautics

John N. Dyer,
Dean of Science and Engineering

ABSTRACT

An experimental investigation was conducted to examine the effects of fuel-air ratios, fuel composition and smoke-suppressant fuel additives on the sooting characteristics of a T-63 combustor. Multiple wavelength light transmission and two-angle light scattering measurements were used to measure the mean soot diameter. Ferrocene, 12% Cerium Hex-Cem and USLAD 2055 were found effective in reducing exhaust gas opacity. Initial results were conflicting on the cause for the reduced opacity.

TABLE OF CONTENTS

LIST OF TABLES

LIST OF FIGURES

ACKNOWLEDGEMENTS

I wish to thank Professor David W. Netzer for imparting his knowledge and sharing his experience as well as being encouraging and patient throughout this thesis research. I would also like to thank my wife Evelyn, for her support and encouragement. Most of all I want to thank God, without whom all this would not have been possible.

I. INTRODUCTION

The maintenance of high performace turbofan/turbojet engines by the U.S. Navy/Air Force is carried out in jet test cells on shore based facilities. These test cells are required to adhere to regulations and guidelines set down by the Environmental Protection Agency regarding emmision of air pollutants. In addition to these federal regulations, local state laws often impose more stringent requirements to curb pollution. These regulations are applicable only while the engine is being tested on the ground but not when the engine is airborne. Therefore, the primary concern is in the control of exhaust products that an engine generates in a post-overhaul test conducted in a test cell.

To comply with the emission regulations, the existing test cells themselves could be modified to treat and regulate the exhaust products from the engine under test. However, this is extremely costly. Another, less expensive, alternative is to modify the fuel itself or the combustion process so that cleaner exhaust products are produced. A study into this alternative has been undertaken by the Naval Postgraduate School. This research is directed at studying the effects of fuel additives and fuel composition on the sooting characteristics within, and exterior to, a T63 engine combustor.

This thesis was a continuation of the work that was initiated by Bennett [Ref. 1], who used light transmission and scattering techniques to measure the particle size and mass concentration of the soot generated in the T63 combustor. Several improvements were made to the test facility used by Bennett in order to improve the quality of data gathered. These improvements included the installation of an air heater to raise the temperature of the incoming air to the combustor in order to simulate more realistic

compressor discharge conditions, the use of laser sources instead of white light sources in the combustion region and the addition of a light chopper and phase-lock amplifiers to prevent combustion light from being measured by the photodiodes. The objective of this study was to determine quantitatively the effects on soot particle size and mass concentration by different smoke-suppressant fuel additives, and fuel compositions at different air inlet temperatures.

II. THEORY

A. LIGHT TRANSMISSION TECHNIQUE

K.L. Cashdollar [Ref. 2] had successfully applied this technique to measure the particle size and mass concentration of a cloud of smoke. The transmission of light through a cloud of uniform particles is given by Bouguer's law [Ref. 2] :

$$T = \exp(-QAnL) = \exp[-(3QCmL/2\rho d)] \qquad \text{(eqn 2.1)}$$

where T = fraction of light transmitted
Q = dimensionless extinction coefficient
A = X-sectional area of particle
n = number concentration of particles
L = path length the light beam traverses
Cm = mass concentration of particles
ρ = density of individual particles
d = particle diameter

A more useful relationship was developed by Dobbins [Ref. 3] for a polydisperse system of particles:

$$T = \exp[-(3Q'CmL/2\rho D32)] \qquad \text{(eqn 2.2)}$$

where Q' = average extinction coefficient
D32 = volume-to-surface mean particle diameter

Using Mie scattering theory, Q' can be calculated as a function of particle size, wavelength of light, complex refractive index of the particle and medium and the standard deviation of the particle size distribution. A log-normal distribution for the smoke particles was used. A computer program was provided by K.L. Cashdollar of the Pittsburgh Mining and Safety Research Center, Bureau of Mines, which produced plots of Q'_λ and Q'_λ ratios (which are both functions of wavelength) versus values of D32. Taking the natural logarithm of equation 2.2 and writing it for a specific wavelength:

$$\ln T_\lambda = Q'_\lambda [-3CmL/2\rho D32] \qquad \text{(eqn 2.3)}$$

Since the three-wavelength detector measures the transmission for all three wavelengths over an identical path through the smoke cloud, the ratio of the logarithm of the transmission (see equation 2.3) at any two wavelengths is equal to the ratio of the calculated extinction coefficients for the same wavelengths:

$$[\ln T_{\lambda 1}/\ln T_{\lambda 2}]=[Q'_{\lambda 1}/Q'_{\lambda 2}] \qquad \text{(eqn 2.4)}$$

With this ratio as the input parameter to the Q'_λ ratio versus D32 plot, the value of D32 can be determined. As the three wavelength measurements yield three ratios, three values of D32 will be obtained. If the refractive index(m) and the size distribution width(σ) are correctly chosen, all three values of D32 obtained from the Q'_λ versus D32 plots will be consistent. If the three values of D32 are not

consistent, either the size of the distribution width or the refractive index or both must be varied. Most of the particulates from the combustion can reasonably be assumed to be carbon. From previous studies [Ref. 2], some refractive indices for carbon are available. In this investigation, a complex refractive index of m = 1.95 - i0.66 was used. The refractive index of surrounding medium was unity for air and the standard deviation of the particle distribution, σ, was taken as 1.5. Once Q'_λ, D32 and T_λ are known, the mass concentration can be calculated from the following rearrangement of equation 2.3:

$$Cm = -[2\rho D32 \ln T_\lambda]/3Q'_\lambda L \qquad \text{(eqn 2.5)}$$

Figures 2.1 to 2.4 show typical plots produced by the Cashdollar program for given values of refraction index (m) and three values of wavelength.

B. FORWARD LIGHT SCATTERING TECHNIQUE

An alternative to the light transmission technique for finding D32 is to measure scattered light. According to Hodkinson [Ref. 4], the ratio of the forward scattered intensities at two scattered angles yields a measure of the particle mean diameter, D32. For a polydisperse cloud, the ratio of intensities at two forward scattering angles θ_1 and θ_2, is given by:

$$I(\theta_1)/I(\theta_2) = F(\theta_1)/F(\theta_2) \qquad \text{(eqn 2.6)}$$

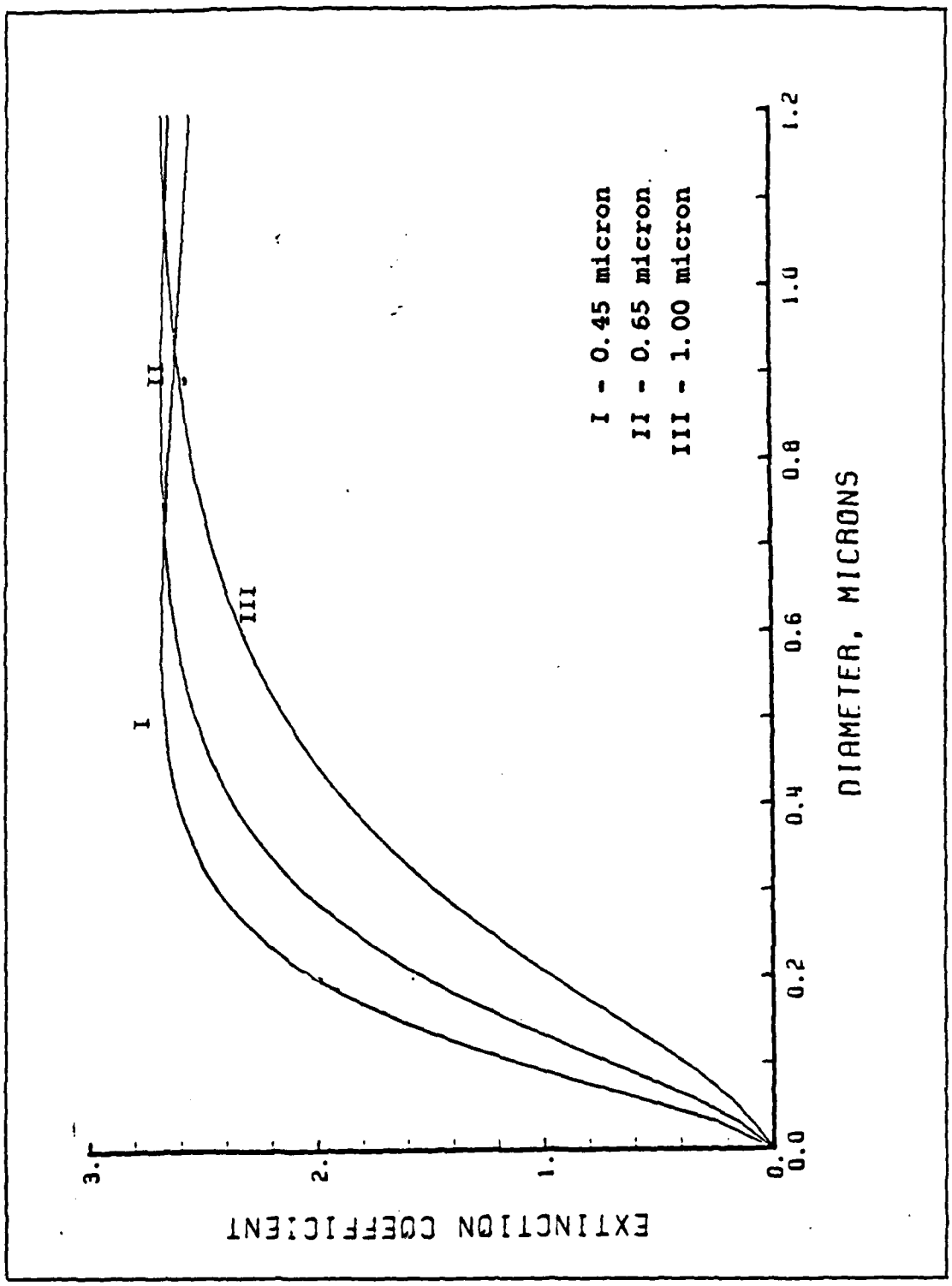

Figure 2.1 Extinction Coefficient versus D32.

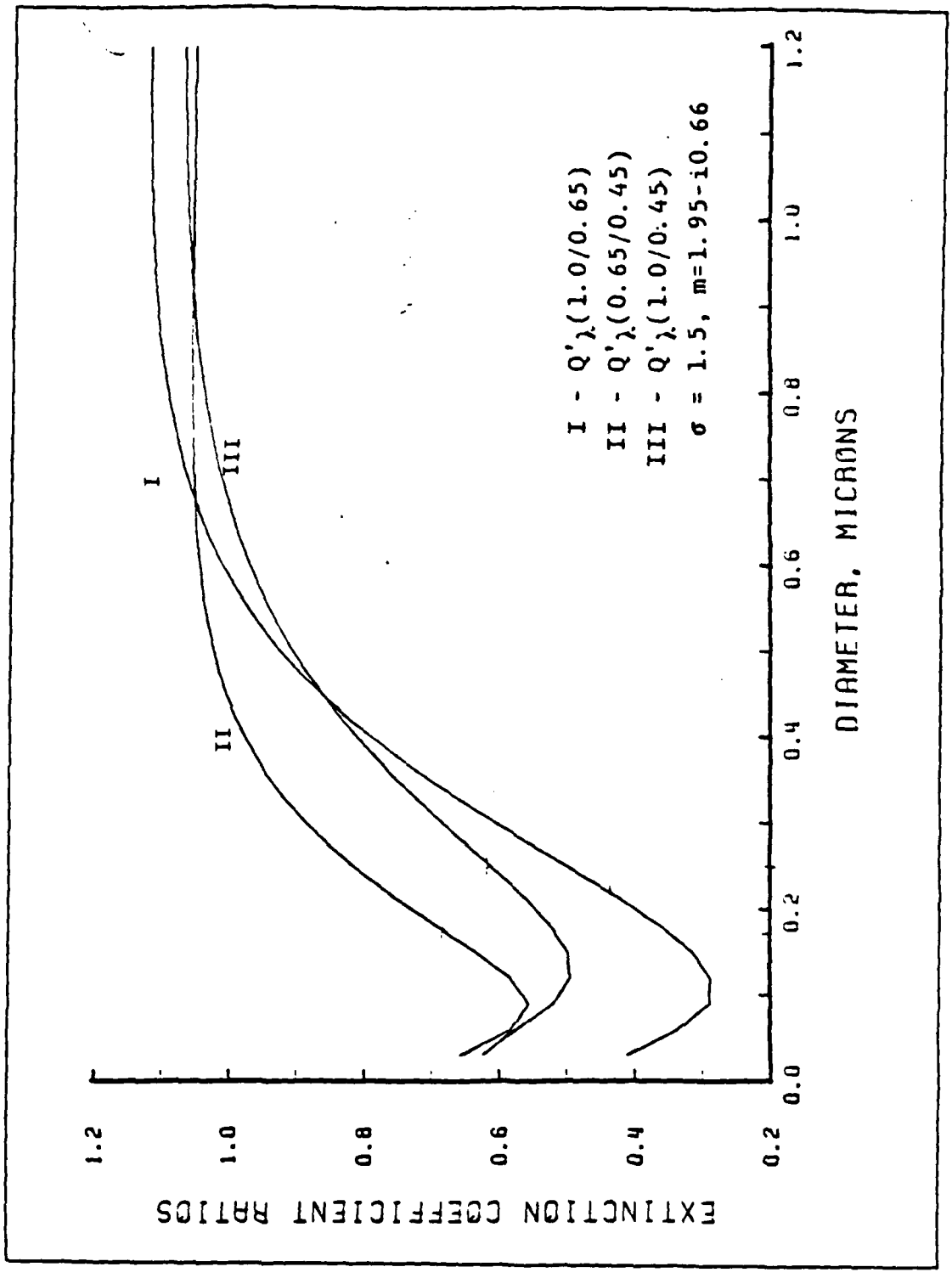

Figure 2.2 Extinction Coefficient Ratios versus D32.

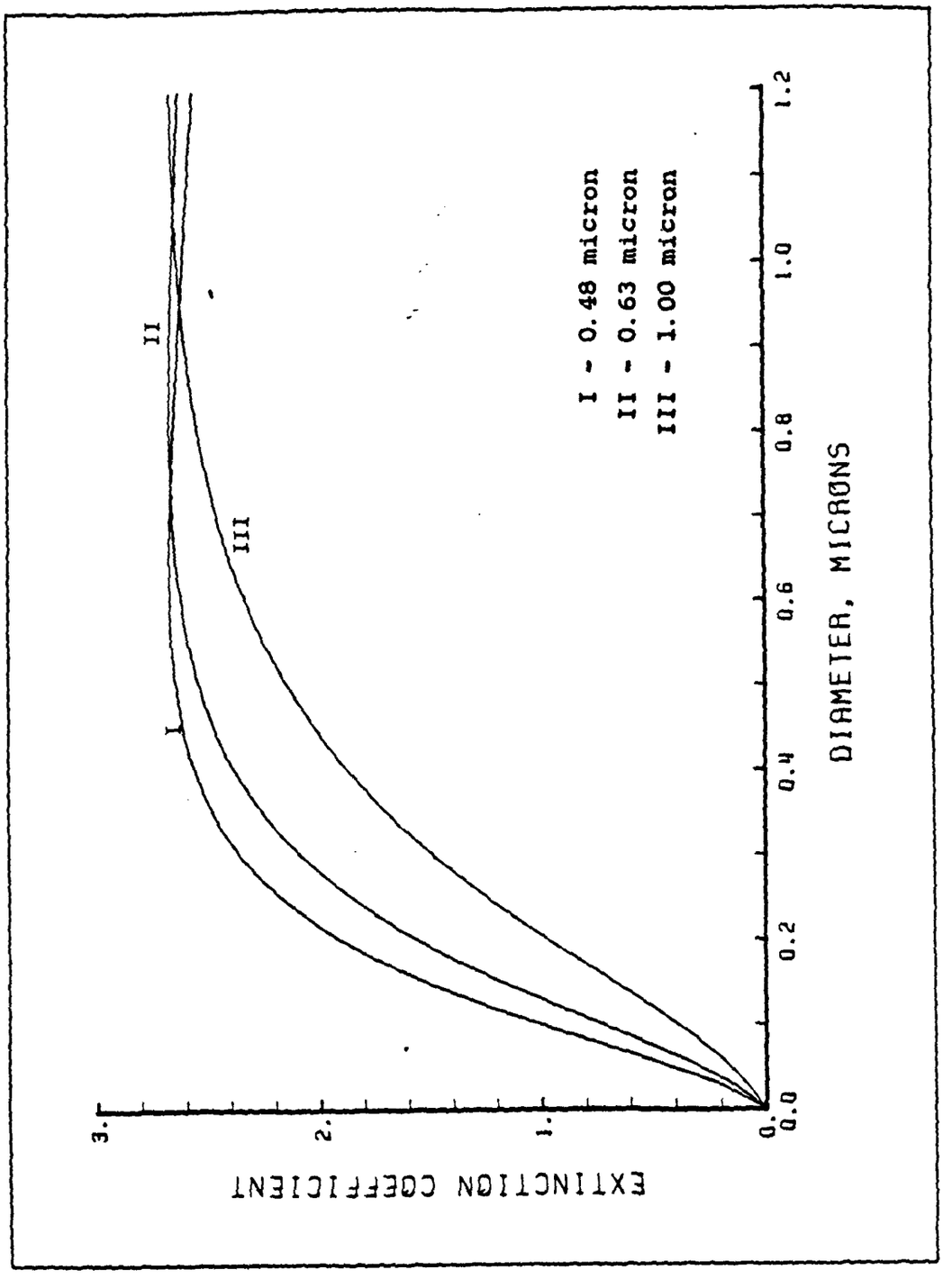

Figure 2.3 Extinction Coefficient versus D32.

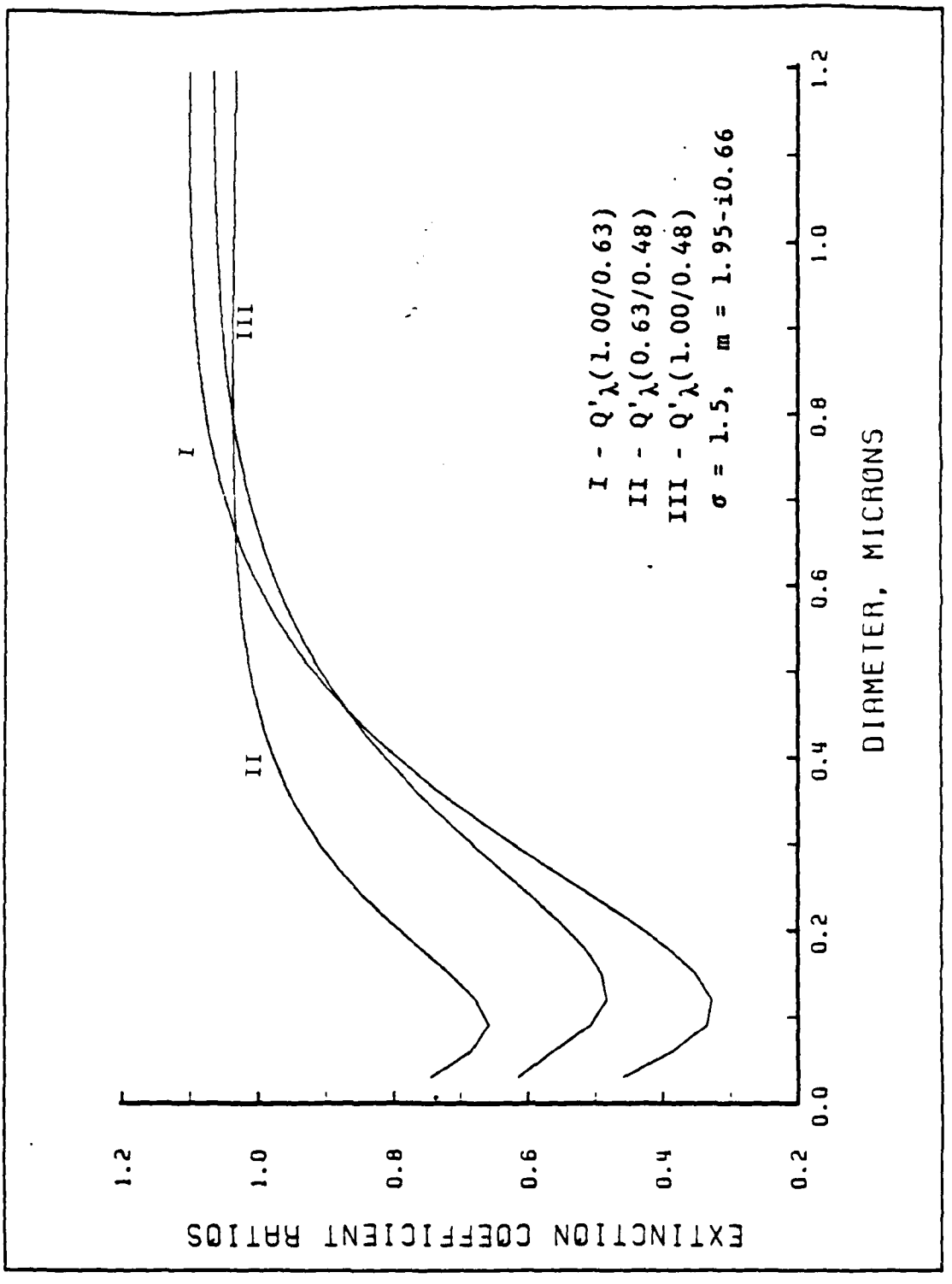

Figure 2.4 Extinction Coefficient Ratios versus D32.

Powell and Zinn [Ref. 5] assumed an upper limit distribution function(ULDF) which gives the following equation for $F(\theta)$ which considers only Fraunhoffer diffraction:

$$F(\theta) = \int(1+\cos^2\theta)[J_1(\alpha\theta\xi)/\alpha\theta\xi]^2 \quad X \quad \exp[-(\delta\ln(a\xi/1-\xi))^2]d\xi/1-\xi \qquad \text{(eqn 2.7)}$$

where,

$$\alpha = \pi Dm/\lambda \qquad \text{(eqn 2.8)}$$

and

$$Dm/D32 = 1 + a\exp(1/4\delta^2) \qquad \text{(eqn 2.9)}$$

where a and δ are adjustable parameters
α = size parameter
Dm = maximum particle diameter
ξ = particle diameter divided by Dm
J_1 = Bessel function of order one

Typical values of a and δ are 1.13 and 1.26 as given by [Ref. 5].

The ratio of scattered light intensities at two forward angles is relatively insensitive to particle refractive index and concentration. This is a consequence of the forward lobe being primarily due to Fraunhoffer diffraction phenomena which are independent of optical properties of the particle (since diffraction arises from light passing near the particle rather than light undergoing reflection or refraction) [Ref. 3]. For given values of α (related to D32 by equation 2.9), angle θ, a and δ, equation 2.7 is readily evaluated by numerical integration, producing a plot of

Intensity ratio versus D32. In this investigation, intensity measurements at 20^0 and 40^0 were taken. In order to have the recorded intensities referenced to the same scattering volume, the intensities most be multiplied by sin θ. The ratio of the intensity at 40^0 multiplied by sin 40^0 to the intensity at 20^0 multiplied by sin 20^0 is then used as entry to the plot, yielding a value of D32. Figure 2.5 shows a typical plot of the intensity ratio versus D32 for a wavelength of 632.8 nm.

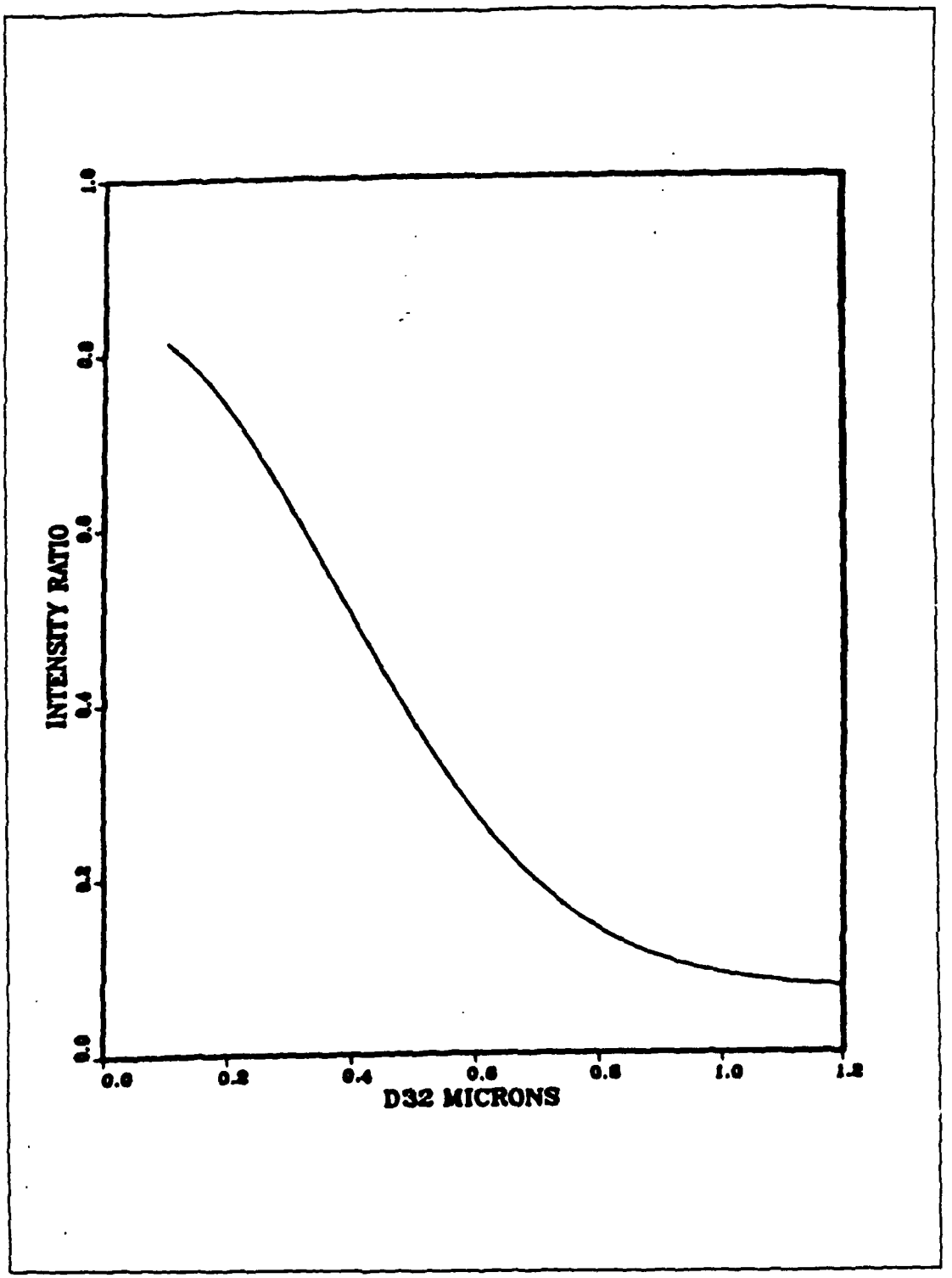

Figure 2.5 Intensity Ratio versus D32.

III. EXPERIMENT DESIGN

In this investigation, a combination of light tranmission and forward light scattering techniques was utilized to measure the particle size D32 and, consequently, the mass concentration (Cm). The D32 determined from light scattering measurements served as a check on the value determined from the light transmission measurements to increase confidence in the data. Figure 3.1 is a schematic of the optical configuration of the experiment.

In the exhaust region of the combustor, white-light from a tungsten source traveled through the smoke cloud to the detector assembly where the beam was split into three parts, each passing through a narrow-pass interference filter to a photodetector. The transmission measurements from these three wavelengths produced three values of mean extinction coefficient ratios. From plots of mean extinction coefficient ratio versus D32 for different diffraction indices of the soot particle, it was possible to determine D32 and the refraction index of the particle. At the same time, scattered light from a He-Ne laser was measured at 20^0 and 40^0 in the exhaust region. With the intensity ratio (multiplied by the $\sin 40^0/\sin 20^0$ to compensate for the difference in scattering volume at the two angles) as input to a plot of intensity ratio versus D32, a second measurement of D32 was obtained. This value was independent of the refraction index of the particle and was also independent of the light transmission measurements.

In the combustion region, two laser sources were used for the light transmission measurement. This yielded one single mean extinction coefficient ratio. With the refraction index determined by the three wavelength measurement from the exhaust region and this single ratio, the plot of

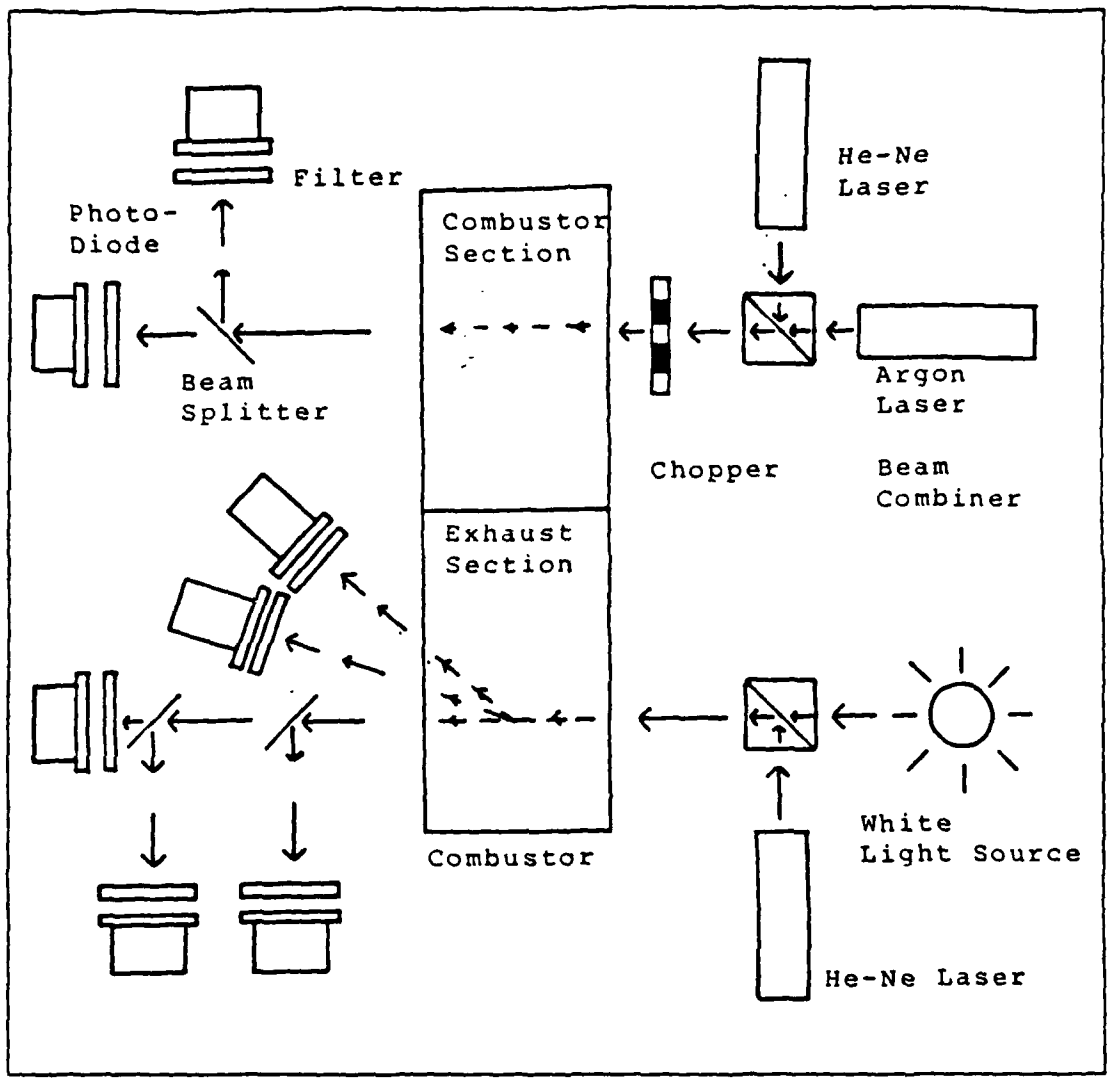

Figure 3.1 Setup of the Optical System to Measure Light and Scattering in the T63 Combustor.

mean extinction coefficient versus D32 gave the value of D32 in the combustion region. It was assumed that the refractive index of the particles remained unchanged as it passed from the combustion region to the exhaust region. Scattered light measurements were to be taken at 20^0 and 40^0 for the He-Ne laser source to yield a second value or D32 as a check against that obtained by the two-laser transmisson

measurement. However, these scattering measurements could not be successfully taken because of the presence of excessive combustion light. Finally, from the value of D32 obtained from the two-laser measurement, the mass concentration was computed.

IV. EXPERIMENTAL APPARATUS

A. COMBUSTOR

A T63-A-5A combustor can was chosen for this experiment because the inlet air demands of this engine were within the compressed air supply capabilities available at the combustion laboratory. This is the same combustor used by Bennett [Ref. 1] except that the four exhaust tubes at the aft end were replaced with a single equivalent-sized nozzle to permit measurements on the exhaust characteristics in a separate experiment. The modified engine is shown in Figure 4.1. Also Figure 4.2 shows the general layout of the air and fuel supplies to the engine combustor.

B. HYDROGEN-FUELED VITIATED AIR HEATER

The air heater previously installed was set to work by the addition of a rod into the airstream just ahead of the air heater ignitor to create a recirculation zone to sustain the heater flame. The following settings were used to achieve an air inlet temperature of 300^0 F:

	Mass Flow Rate (lbm/s)	*Sonic Choke Pressure(Psia)*	*Sonic Choke Diameter(in)*
Air	1.9	595	0.420
Hydrogen	0.0032	420	0.040
Makeup Oxygen	0.026	233	0.076

C. LIGHT TRANSMISSION MEASURING APPARATUS IN THE COMBUSTION REGION

Originally, the same equipment used by Bennett [Ref. 1], viz., a projector light source, was used for carrying out light transmission measurements in the combustion region.

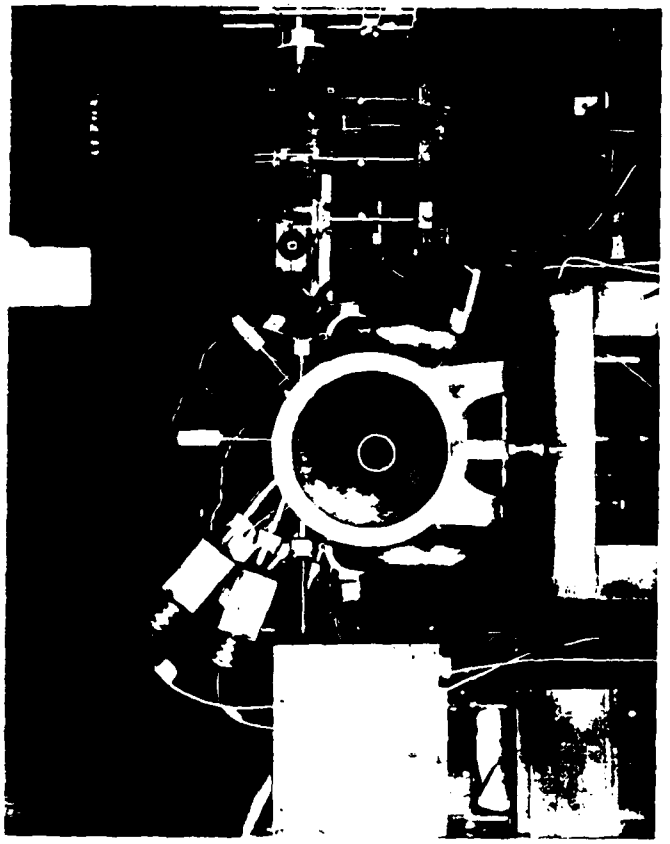

Figure 4.1 Modified T63 Combustor.

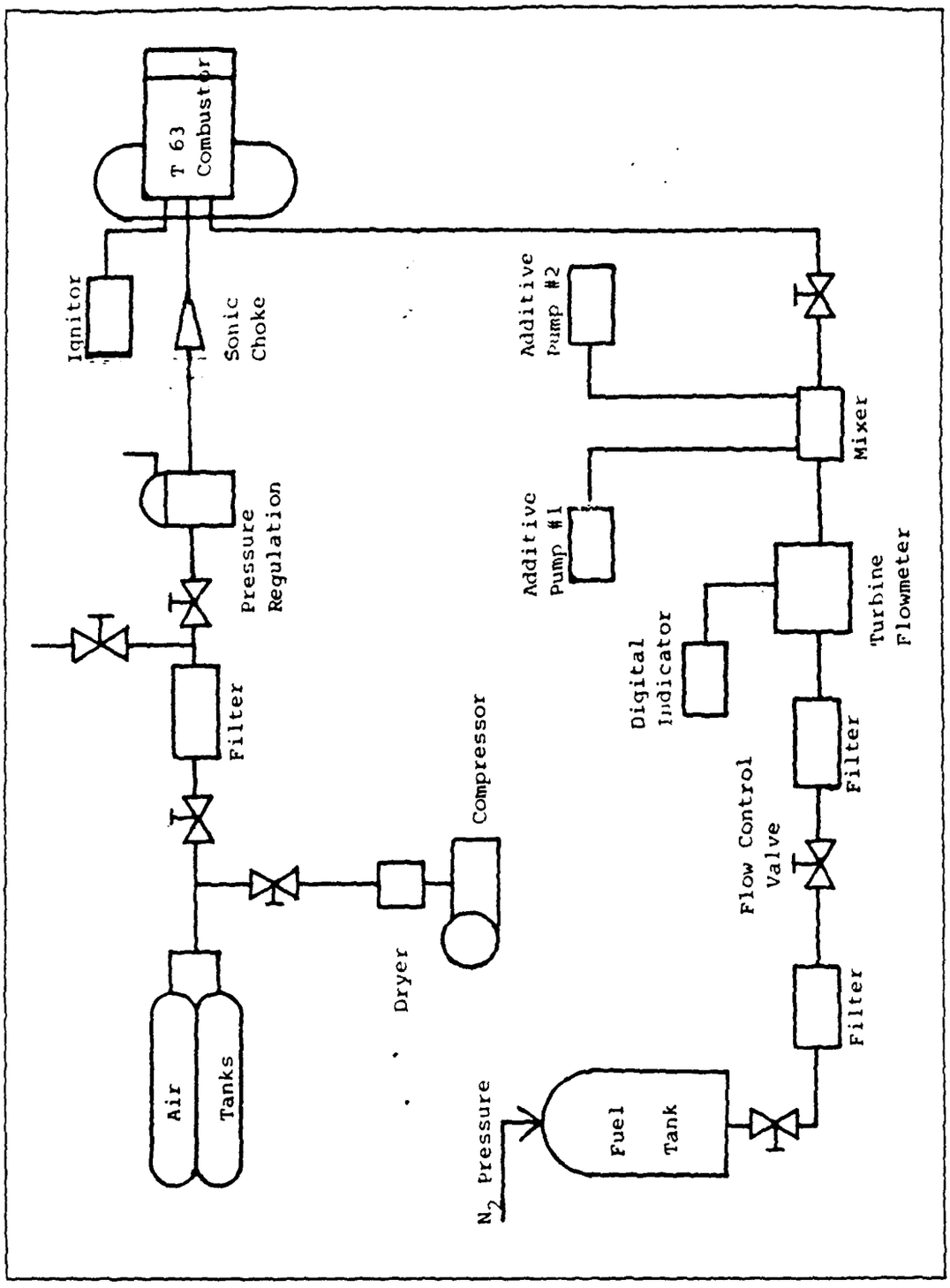

Figure 4.2 Schematic of Air and Fuel Systems in the Experiment Setup.

However, results from several tests showed that the amplitude of the projector light through the smoke cloud was overwhelmed by the combustion light present in that region. As a result, the transmitted light was lost and became indistinguishable. It was also felt that the "light-on", "light- off" technique used by Bennett was not accurate enough due to the magnitude of the combustion generated light in comparison to the projector light source. This did not permit a transmittance calculation to be made. The projector light source was then replaced by 2 lasers, an Argon laser operating at 488.0 nm and a He-Ne laser operating at 632.8 nm. These sources, being significantly more intense, were able to be detected through the smoke cloud despite the combustion light. A light chopper was added to further distinguish the laser light from the combustion light. The light chopper, operating at 90 Hz, was placed in the laser path before entering the combustor. The photodiode detector outputs (containing both the combustor and laser light) were passed through a phase-lock amplifier which was synchronized with the chopper. The phase lock amplifier produced an output which was proportional to the chopped light signal. In addition, laser line filters were installed in the photodiode detectors to help filter out combustion light. Before actual data was taken, several trial tests to evaluate the effectiveness of this setup were carried out and the results showed that the combination of light chopper, phase lock amplifier and laser line filters did eliminate the influence of combustion light on the transmittance readings. Figures 4.3, 4.4 and 4.5 shows the setup of the lasers and white- light source in the experiment. Figure 4.6 shows the three photodiodes housed in the transmittance detector box. Only two of the three detectors in the box are used for the laser light transmissions in the combustion region. Figure 4.7 shows the light paths traversed by the

laser sources in the combustion region. Attempts to measure scattered light at 20^0 and 40^0 in the combustor region failed as there was too much combustion light present in comparison to the low intensities of the scattered light. The signal-to-noise ratio was too low to be distinguished by the phase-lock amplifiers. Therefore, only transmittance measurements were carried out in the combustion region.

D. LIGHT TRANSMISSION AND SCATTERING MEASURING APPARATUS IN THE EXHAUST REGION

As the problem of combustion light interfering with the transmittance measurement did not exists in the exhaust region, a projector-type light source was used here. The transmitted light entered the photodiode detector box and was split into three paths by beam splitters. These three beams were collected individually by three photodiodes which had filters of 450 nm, 650 nm, and 1014 nm respectively. This is shown in Figure 4.7. For light scattering measurements in the exhaust region, a He-Ne laser beam at 632.8 nm was used and the photodiode detectors were positioned at 20^0 and 40^0 to collect the scattered light. Figure 4.8 is a schematic showing the light paths in the exhaust section of the combustor.

E. TEMPERATURE MEASURING APPARATUS

Four sheathed chromel-alumel thermocouples were radially located in the combustor to monitor the temperature profile around the combustor. These thermocouples were connected by chromel-alumel wires directly to the data acquisition system. The positions of the thermocouples on the combustor are shown in Figures 4.9 and 4.10 . These thermocouples could be used in conjunction with the water-cooled probe which traversed the combustor centerline.

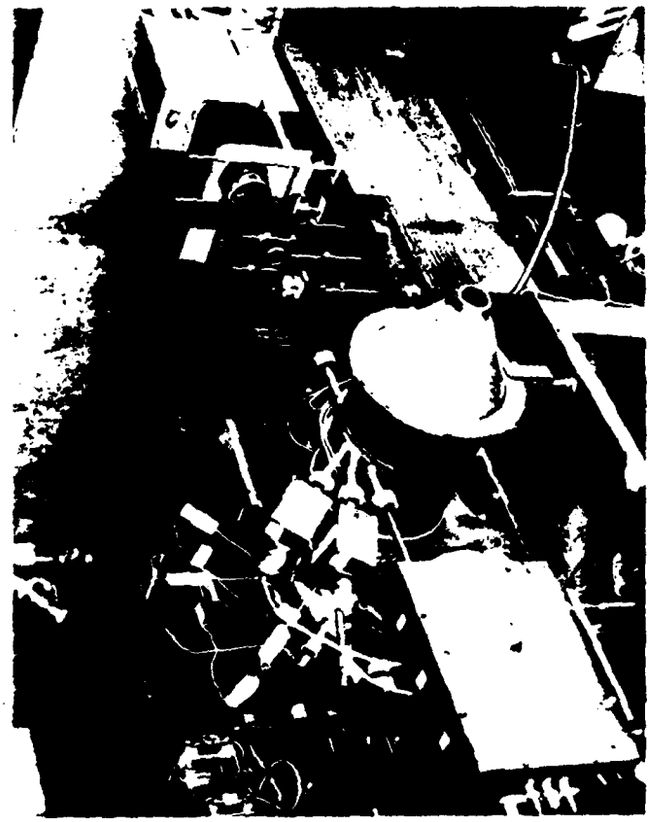

Figure 4.3 Combustor with Measuring Apparatus Fully Set Up.

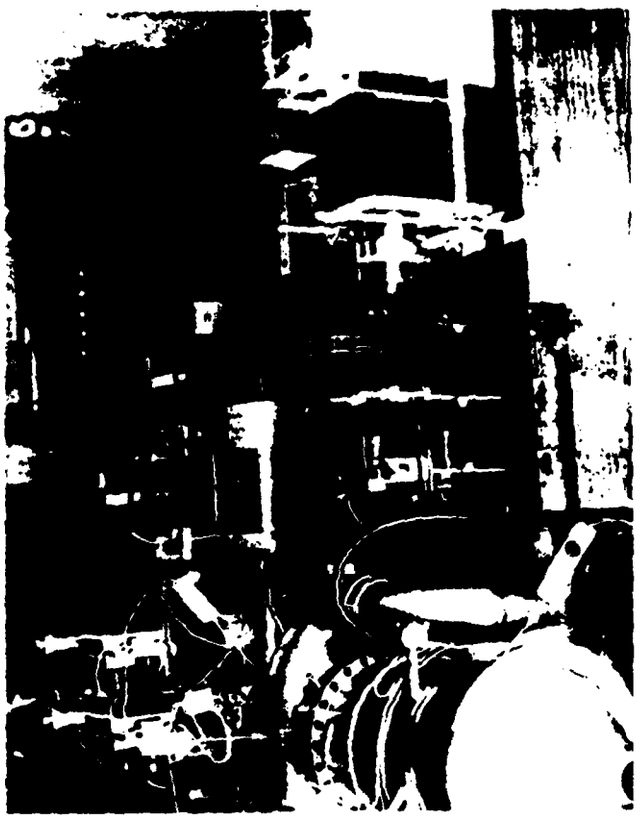

Figure 4.4 Close-up View of Laser Systems.

Figure 4.5 Another View of Combustor with Measuring Apparatus Fully Set Up.

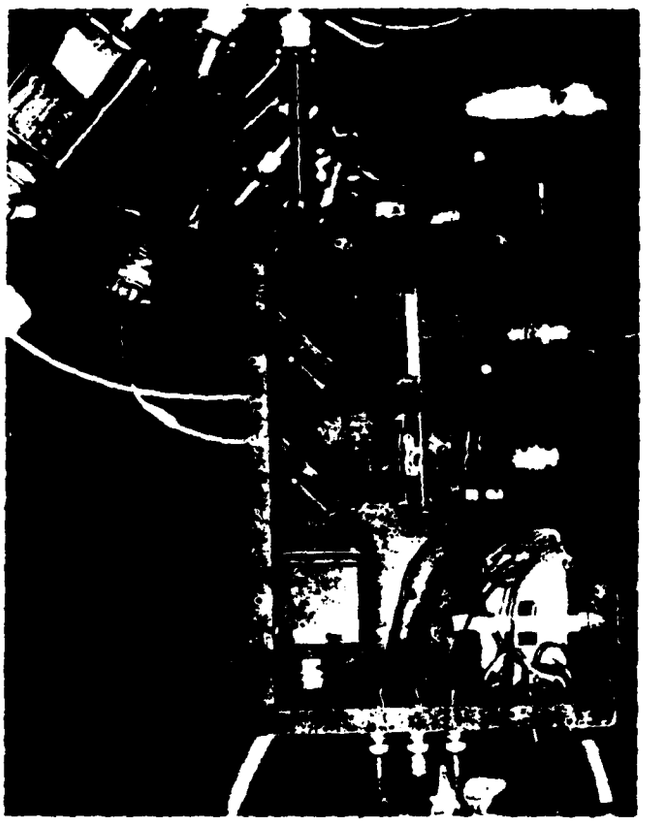

Figure 4.6 Photodiodes in Detector Box.

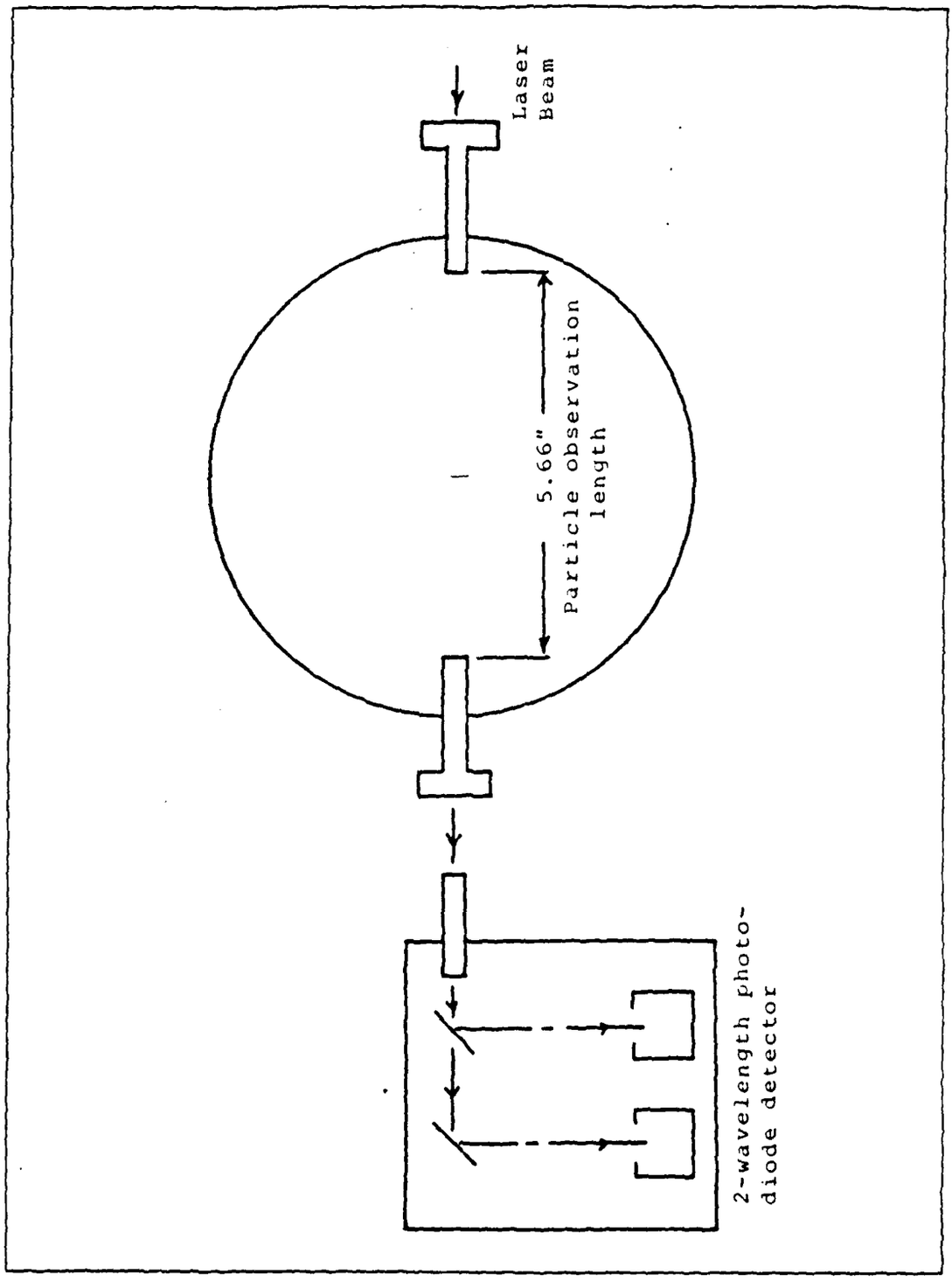

Figure 4.7 Schematic of Light Paths in Combustion Region.

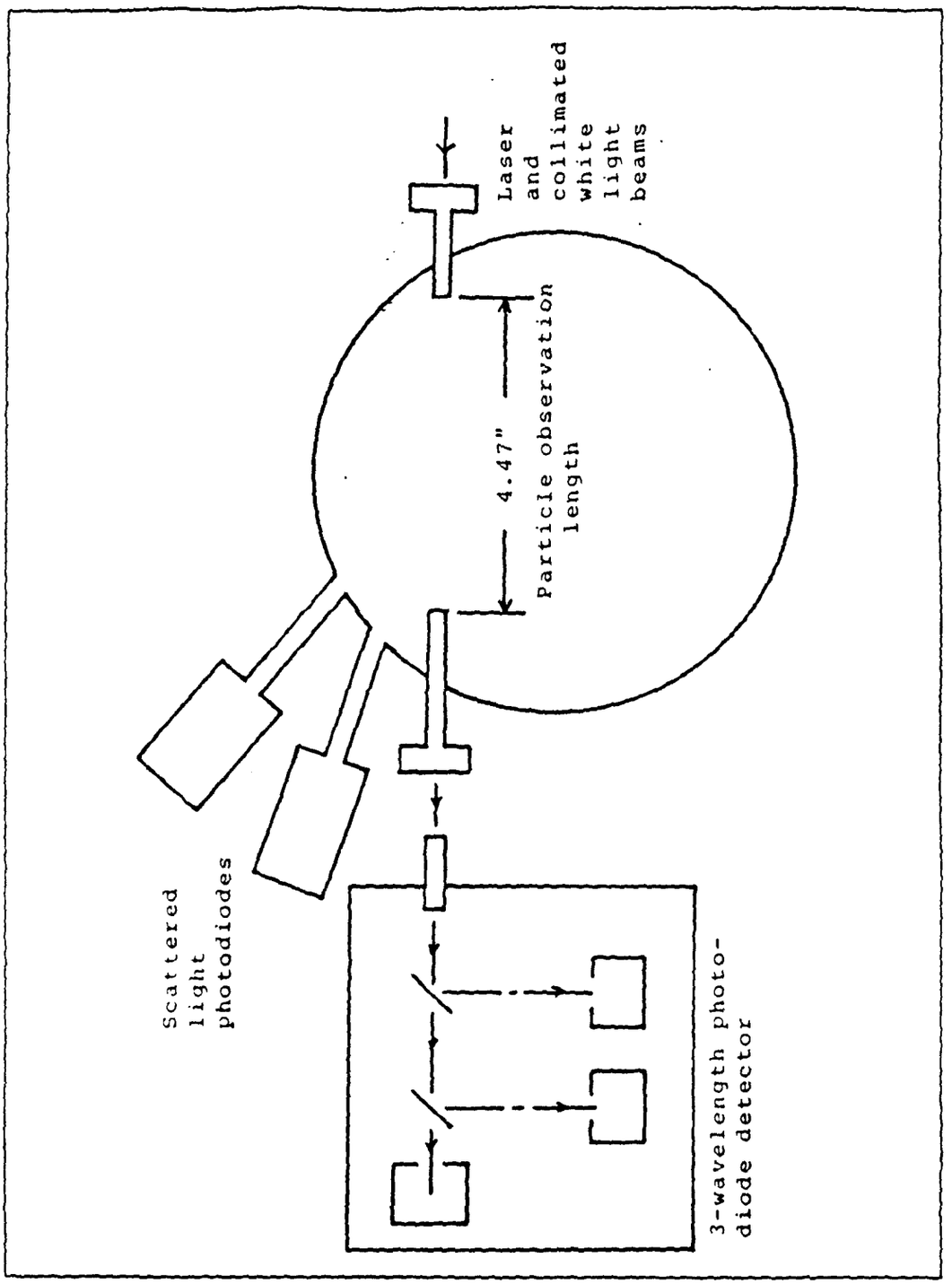

Figure 4.8 Schematic of Light Paths in Exhaust Section.

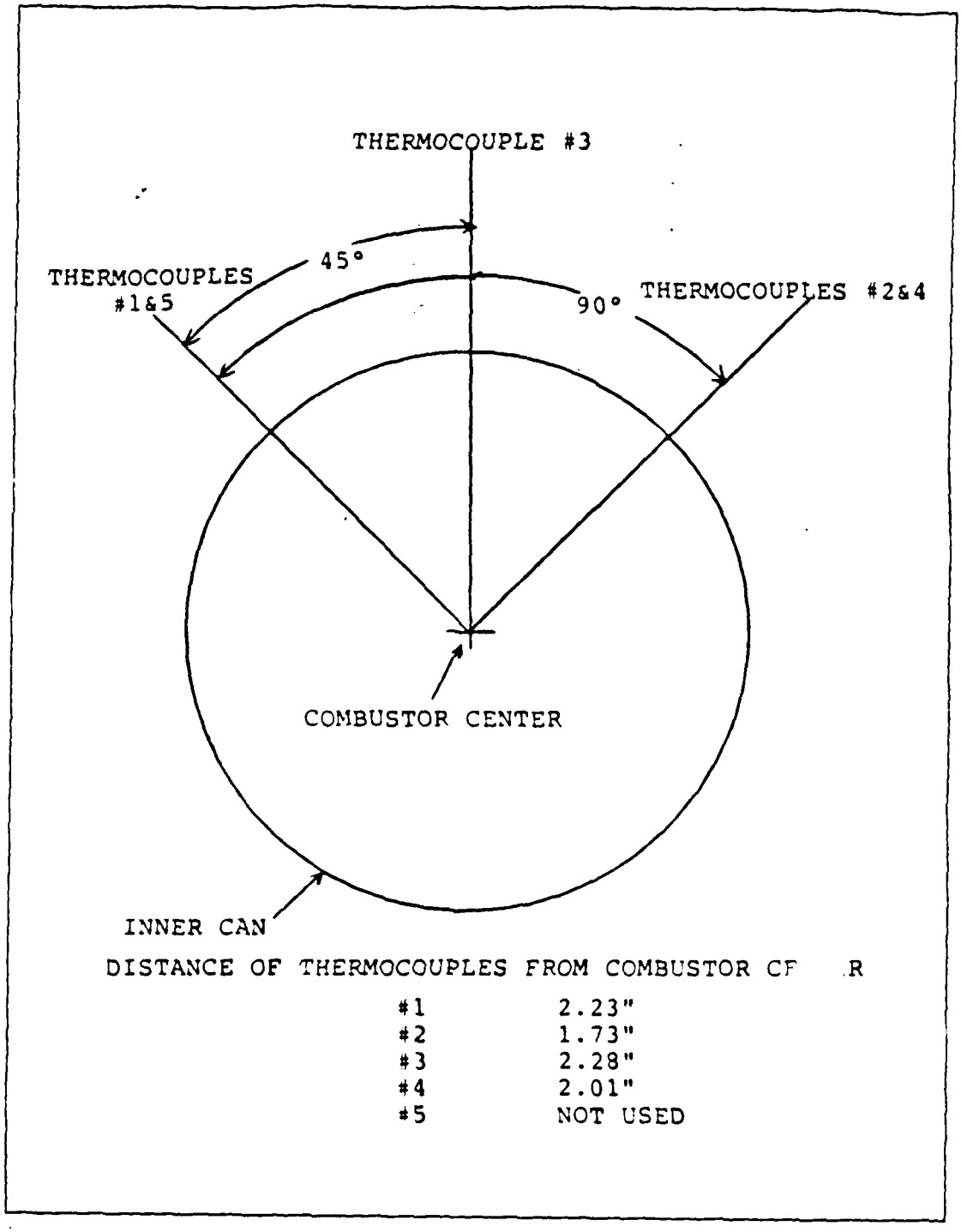

Figure 4.9 Thermocouple Placement (side-view).

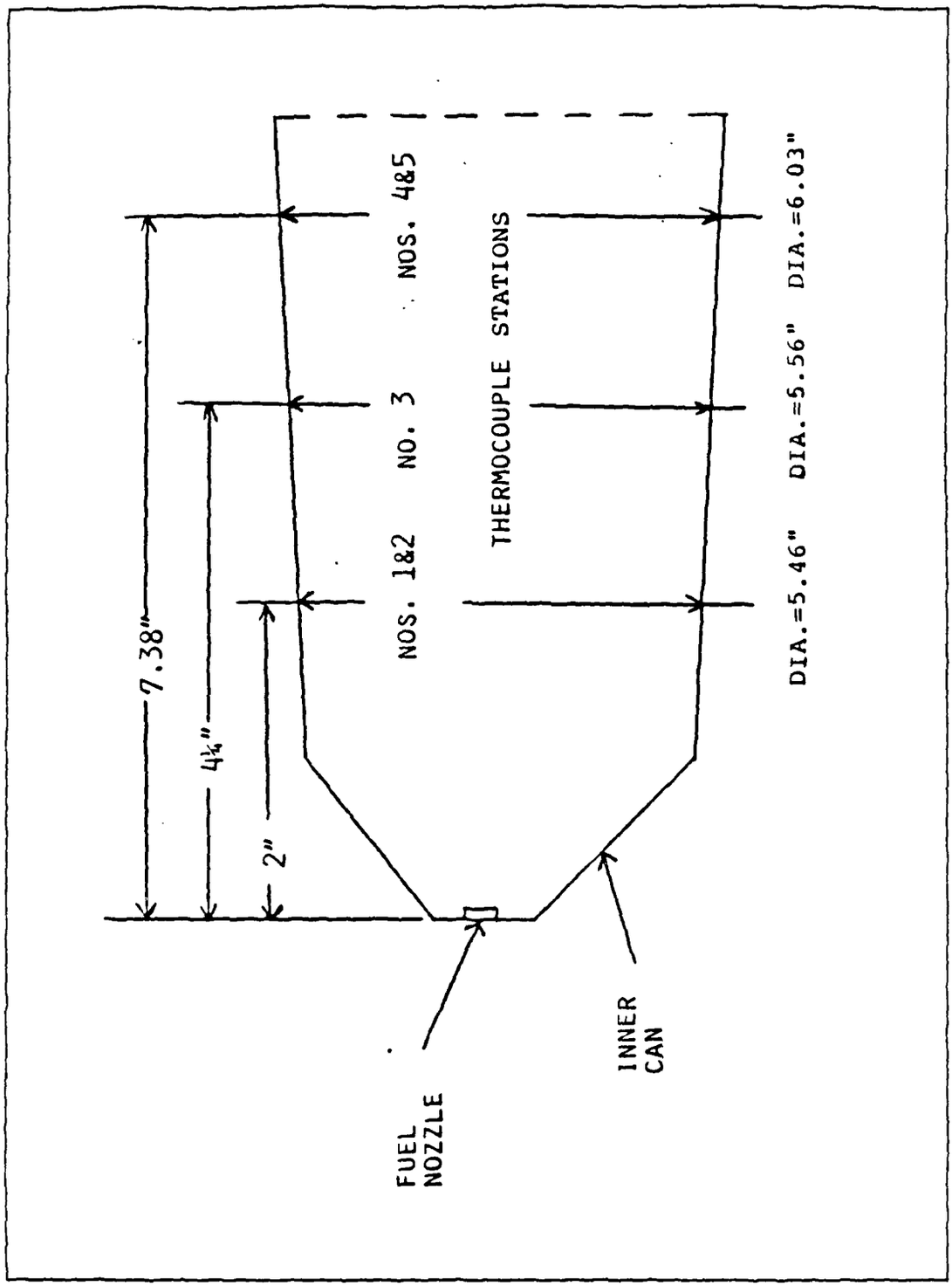

Figure 4.10 Thermocouple Placement (end-view).

F. CONTROL PANEL AND DATA CAPTURING

All tests were conducted from the control room where the main air supply, fuel flow rate and fuel additive flow rate could be controlled. Main air into the combustor was controlled by a dome loaded pressure regulator, and a solenoid operated on-off valve and a sonic choke. Fuel flow was controlled by a throttle valve and measured with a turbine flowmeter. Two precision metering pumps which controlled the fuel additive flow rates were operated by a switch on the control panel. Additive volume consumed was determined by measuring the amount of additive in the reservoir before and after the pump operation. Flow rate was then calculated using the elapsed time of pump operation. Mixing of additive and fuel was accomplished by a swirl-type mixer. Figure 4.11 shows the T-63 control panel. All data were recorded by a Hewlett-Packard HP9836 data acquisition system. This is shown in Figure 4.12 .

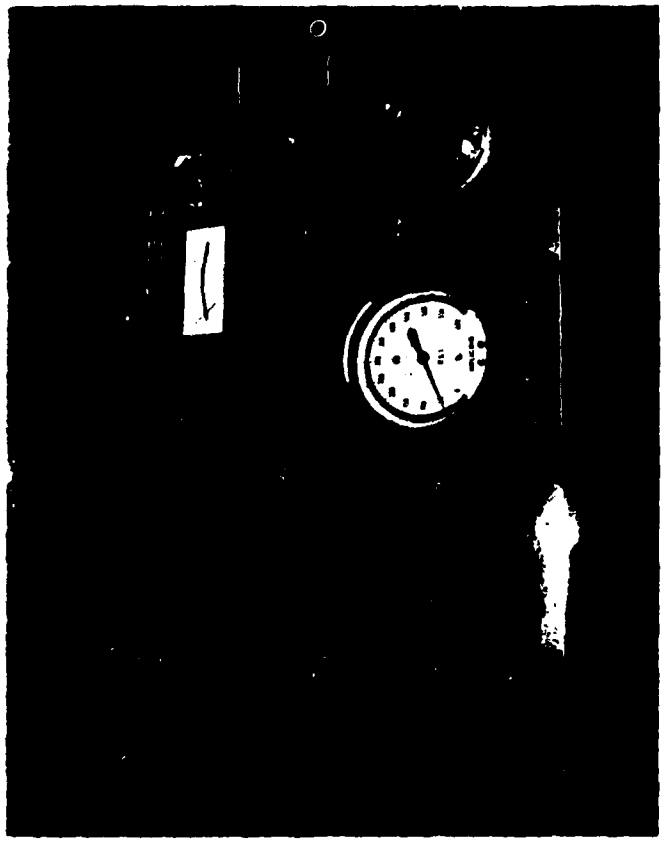

Figure 4.11 Control Panel.

Figure 4.12 Data Acquisition System.

V. EXPERIMENTAL PROCEDURE

Before each run, the data acquisition/reduction program was loaded into the computer and then all pressure transducers were calibrated with a dead-weight tester. Alignment between the laser beams/light source and the photodiode detectors were also checked. All manual air and fuel valves were required to be opened. The fuel tank was pressurized and the nitrogen supply to operate the control panel was turned on. In each test, a sequence was executed by the computer program to collect four different sets of data. These were 'No Ignition', 'Ignition-Fuel Only', Ignition-additive' and 'Post No-Ignition' data sets. The first refers to measurement of parameters in the engine without the engine being ignited but with air flowing. The second and third data sets refer to the measurements taken when the engine was ignited with fuel and fuel with additive respectively. The fourth data set was taken when the engine was shut down and only air was flowing. In each data set, the following were measured:

- fuel flow rate
- pressure of heater fuel
- pressure of make-up oxygen
- pressure of main air
- chamber pressure
- main air temperature
- inlet air temperature
- heater fuel temperature
- make-up oxygen temperature
- radial thermocouple temperatures
- voltages from the photodiodes for the transmitted light
- voltages from the photodiodes for the scattered light

Exhaust temperature was simultaneously captured by the data acquisition and monitored on a strip chart recorder during each test. This was done so that visual monitoring could be accomplished during the test. From the measured parameters, gas flow rates were calculated.

VI. RESULTS AND DISCUSSION

In this investigation, NAPC #7 fuel was tested at six different fuel-air ratios. In addition, the effects of three smoke suppressant fuel additives, viz., Ferrocene, 12% Cerium Hex-Cem and USLAD 2055 were tested using the NAPC #7 fuel. Two tests were also carried out using NAPC #3 fuel. The properties of NAPC #3 and #7 fuel are shown in Table 1. Fuel #7 was higher in aromatic content and lower in hydrogen than fuel #3. Fuel additive and fuel-air ratio effects on mean soot diameter, soot concentration and opacity are discussed below:

A. EFFECTS OF DIFFERENT FUEL-AIR RATIOS USING NAPC #7 FUEL (RUNS #1- #12)

The results of the tests are shown in Tables 2 and 3. The strip chart recordings for the runs are shown in Figures 6.1 to 6.11. It was difficult to fully utilize the computer acquired output from the three-wavelength light detectors. This was due primarily to the necessity for manually observing the proper post-run time for recording the "air-only" 100% transmittance values. For this reason, the exhaust transmittance values were also recorded on strip chart recorders. The forward measurement location utilized only two wavelengths. The light-chopper/phase lock amplifiers used at this location, together with the index of refraction of soot determined at the aft location, permitted data to be successfully recorded by the computer. The following are comments pertaining to runs #1-#12:

- Run #1 - The strip chart recordings for this run were not obtained and the transmittances were determined only from the data acquisition system.

TABLE 1
PROPERTIES OF NAPC #3 AND #7 FUEL

	NAPC #3	NAPC #7
API Gravity @ 15°	41.3	35.6
Distillation (ASTM) IBP °c	171	193
RECOVERED 10% MAX	192	204
RECOVERED 20%	203	209
RECOVERED 50%	227	226
RECOVERED 90%	261	272
End Point, °c, max	276	288
RESIDUE (ML), MAX	1.4	3.6
LOSS (ML), MAX	0.1	0.4
COMPOSITION AROMATICS (VOL%), MAX	22.8	26.4
OLEFIN (VOL%), MAX	0.75	0.86
HYDROGEN CONTENT (WT%), MIN	13.66	12.83
ANILINE - GRAVITY PROD., MIN	5811	4254
Freeze Point, °C	-34	-31
Viscosity @ 37.8°C, (cSt)	1.62	1.77
Temperature @ 12 cSt, (°C)	-35.6	-30.6

TABLE 2

RESULTS OF TESTS ON NAPC #7 AND #3 FUELS

Run no.	Exhaust Temp (°R)	f	Combustion Region Transmittance T(0.48)	T(0.63)	D32 (micron)	Exhaust Region Transmittance T(1.0)	T(0.65)	T(0.45)	D32 (micron)
1	1790	.0163	.250	.140	.17	.888	.782	.675	.170
2	1630	.0156	.247	.176	.20	.830	.727	.616	.180-.210
3	1754	.0154	.260	.136	.10	.868	.760	.671	.180-.190
4	1530	.0141	.268	.200	.21	.83	.74	.650	.180-.260
5	1530	.0140	.270	.179	.18	.847	.763	.673	.180-.230
6	1630	.0150	.204	.144	.21	.845	.750	.662	.190-.215
6a	1643	.0148	.218	.145	.19	.858	.761	.671	.185-.205
7	1635	.0154	.264	.144	.13	.847	.725	.664	.170-.220
7a	1642	.0153	.274	.151	.13	.874	.761	.709	.170-.225
8	1594	.0145	.255	.176	.19	.847	.765	.670	.180-.250
8a	1580	.0143	.281	.188	.18	.88	.810	.730	.180-.230

6a,7a - Ferrocene

8a - 12% Cerium Hex

- Runs #4,5,7,8 and 10 yielded D32 values with a large uncertainty, although the strip chart recordings appeared good and steady readings were obtained. The large uncertainty could be due to changes in the soot particle distribution resulting from running the combustor at such lean fuel-air ratios and low air mass flow rates. The light transmission technique was applicable only to mono-modal, log-normal distributions. In earlier investigations [Ref. 6] in which the combustor was operated at its design air flow rate of 2.65 lbm/sec (vs 1.75 lbm/sec in the present study) the particle diameter measurements were more accurately determined.

TABLE 3

RESULTS OF TESTS ON NAPC #7 AND #3 FUELS

Run no.	Exhaust Temp (°R)	f	Combustion Region Transmittance T(0.48)	T(0.63)	D32 (micron)	Exhaust Region Transmittance T(1.0)	T(0.65)	T(0.45)	D32 (micron)
9	1635	.0154	.265	.172	.17	.852	.759	.667	.180-.200
9a	1641	.0152	.297	.187	.16	.879	.805	.728	.190-.200
10	1632	.0150	.325	.162	*	.851	.762	.670	.170-.220
10a	1640	.0149	.337	.168	*	.886	.809	.730	.180-.200
11	1664	.0156	.09	.189	.14	.845	.788	.660	*
11a	1690	.0156	.14	.240	.16	.876	.831	.715	*
12	1632	.0156	.140	.230	.18	.850	.79	.670	*
12a	1628	.0154	.165	.245	.16	.870	.83	.720	*
13	1764	.0142	.560	.350	*	.878	.774	.698	.150-.180
13a	1760	.0141	.523	.359	*	.918	.838	.790	*
14	1669	.0171	.270	.190	.12	.853	.765	.694	.200-.240
15	1749	.0183	.240	.190	.10	.842	.735	.668	.210-.220

9a,10a - 12% Cerium Hex
11a,12a - USLAD 2055
13a - 12% Cerium Hex

- Run #10 did not provide a D32 value for the combustion region. This was because the extinction coefficient ratio obtained from the experiment resulted in a value off the curve of the extinction coefficient ratio versus D32 plot.
- Runs #11 and #12 gave good exhaust transmittance readings (see Figures 6.10 and 6.11) but the computed extinction coefficient ratios did not result in proper values for entry into the plots to obtain a D32 value (see discussion above for runs #4, etc.).

A plot of the mean values of measured exhaust D32 values versus fuel-air ratio is shown in Figure 6.15. Figure 6.16 is a plot of D32 versus exhaust temperature. The data indicate that as fuel-air ratio (or exhaust temperature) was increased, D32 values decreased. A plot of transmittances versus exhaust tempersture is shown in Figure 6.17. The transmittances were fairly constant with exhaust temperature. This finding is different from earlier findings with higher air flow rates [Ref. 6] which concluded that transmittance decreases as exhaust temperature increases.

B. EFFECTS OF FUEL-ADDITIVES ON NAPC #7 FUEL (RUNS #6A - #12A)

The results are shown in Tables 2 and 3 and the strip chart recordings are shown in Figures 6.5 to 6.11. Runs #10a did not yield a D32 value for the combustor region for the same reasons given above. Runs #11a and #12a were similar to runs #11 and #12 and therefore did not provide a D32 value for the exhaust section as discussed above. In Table 4, it is observed that transmittance increased with the use of additives, although D32 values did not change significantly (see Figure 6.15). The additives also had insignificant effects on exhaust temperatures (see Figure 6.16). Computed mass concentrations (see Table 4) in the combustor exhaust showed significant reductions of soot mass concentration (Cm) with the additives. 12% Cerium Hex-Cem resulted in a 20%-25% reduction in Cm as compared to 16% for Ferrocene. The reduction in Cm for USLAD 2055 was not computed because a D32 was not available. However, the percentage reduction in exhaust transmittance for USLAD 2055 was seen to be between that of Ferrocene and 12% Cerium Hex-Cem, which was the highest.

TABLE 4

% CHANGES IN CM AND EXHAUST TRANSMITTANCES

Run no.	Mass Concentration (mg/litre)	Amount of Additive Used (ml/gal)	% reduction in Cm	% reduction in Exhaust Transmittance T(1.0)	T(.65)	T(.45)
6	.354					
6a	.347	22.8	1.9	1.5	1.41	1.36
7	.368					
7a	.309	30.0	16.0	3.2	4.9	6.7
8	.360					
8a	.270	58.0	25.0	3.9	5.9	8.9
9	.356					
9a	.279	58.0	21.6	3.2	6.0	9.1
10	.35					
10a	.28	58.0	20.0	4.1	6.2	8.9
11	--					
11a	--	--	--	3.6	5.5	8.3
12	--					
12a	--	--	--	2.3	5.1	7.4
13	.361					
13a	.241	58.0	34.5	4.5	8.2	13.2

C. EFFECTS OF COMBUSTOR INLET AIR TEMPERATURE USING NAPC #7 FUEL (RUNS #13 AND #13A)

Combustor inlet air at 270^0F was used in this run. For the additive run (run #13a), the extinction coefficient ratios could not be obtained (see Table 3). However, the ratios were quite close to those obtained for the non-additive run. Therefore, the same D32 value obtained for the non-additive run was used to compute a Cm for the additive

run. The percentage reduction in Cm was 34.5% (see Table 4). This was higher than any of the changes observed when using cold inlet air. The percentage increase in transmittances were also much higher than those measured using cold air. In Figure 6.15, it appears that the increased inlet air temperature caused a significant reduction in D32, but in Figure 6.16 it is seen that at the same exhaust temperature, the particle size change followed the same trend as the cold run data. It is seen that D32 in the exhaust was primarily a function of exhaust temperature. As exhaust temperature increased, D32 decreased. Also in Figure 6.18 are plotted the D32 values from the combustor section. Comparing Figure 6.18 with Figure 6.16, we see that in the combustor, particle size changed more rapidly with fuel-air ratio (or exhaust temperature). At low fuel-air ratios (or exhaust temperature) the particle size in the combustor and in the exhaust duct were nearly identical. As the fuel-air ratio was increased, the combustor particle diameter decreased more rapidly than in the exhaust duct. Thus, there was a growth in mean particle diameter from the combustor to the exhaust duct at high fuel-air ratios.

D. TESTS USING NAPC #3 FUEL (RUNS #14 AND #15)

Two tests (without additives) were carried out using NAPC #3 fuel. The results are shown in Table 3 In Figures 6.15 and 6.16, we see that larger values of D32 were obtained compared to NAPC #7 fuel. Also, in Figure 6.19, where exhaust temperature is plotted against fuel-air ratio, we see that fuel type had an effect on the Te versus f plot. Both of these results are also different from the earlier findings [Ref. 6] which had found no effect of fuel type on Te or D32. However, the earlier experiments were carried out under a different set of operating conditions and this might

be the reason for the difference in findings. The different operating conditions are given below:

	Air Mass Flow Rate (lbm/sec)	Chamber Pressure (lb/in^2)
earlier tests (Ref. 6)	2.65	105
present investigation	1.75	85-90

On the average, the D32 values in the present investigation also had more uncertainty than in the earlier tests.

E. COMPARISION OF RESULTS WITH LIGHT SCATTERING MEASUREMENTS

Runs #1 through #15 were carried out without the light scattering apparatus at the exhaust section being used. The reason was a follows. To operate the light scattering apparatus, a beam combiner was required to be placed in the path of the incident beam for light transmittance measurement. This reduced the intensity of the incident beam to a level where the photodiode was not as sensitive, producing poor results. Therefore, to make a comparison between results from the two different measuring techniques, a separate run using just the scattering apparatus was carried out. The results below showed that there was a reduction in particle size with the use of 12% Cerium Hex-Cem. Also the measured value of D32 was larger than that obtained with the light transmittance technique.

Exhaust Temp (^0R)	Scattering Intensity(20^0) (volts)	Scattering Intensity(40^0) (volts)	Additive Used (ml/gal)	D32 (micron)
1643	0.100	0.035	--	.260
1684	0.073	0.030	58 (Cerium)	.175

The D32 value obtained with additive was in agreement with the light transmission measurement value (see Figure 6.16). The D32 without additive was quite large and may have resulted from measurement error. Further efforts are required to clarify the reasons for these differences obtained using the two optical techniques for particle sizing.

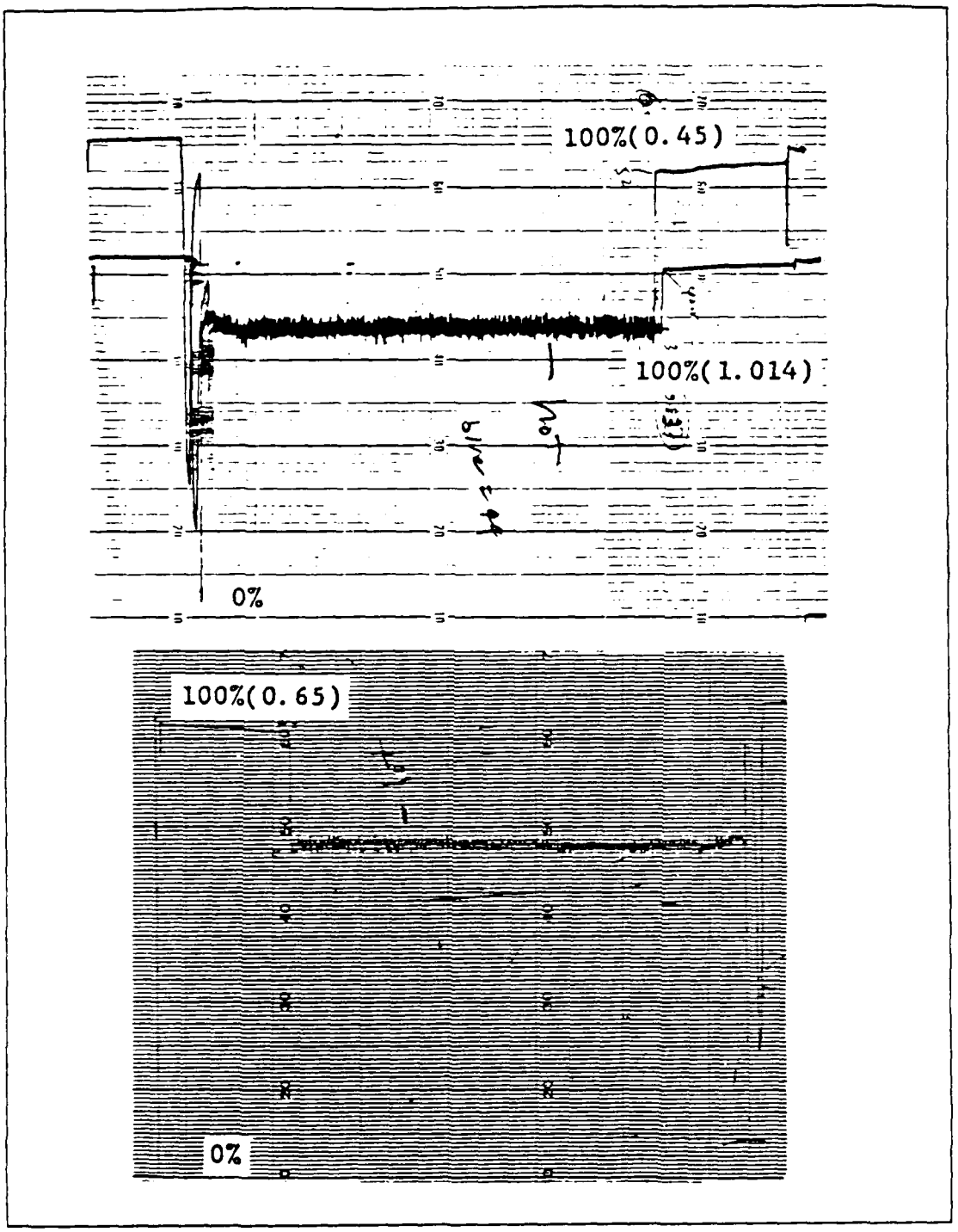

Figure 6.1 Strip Chart Recording of Run #2.

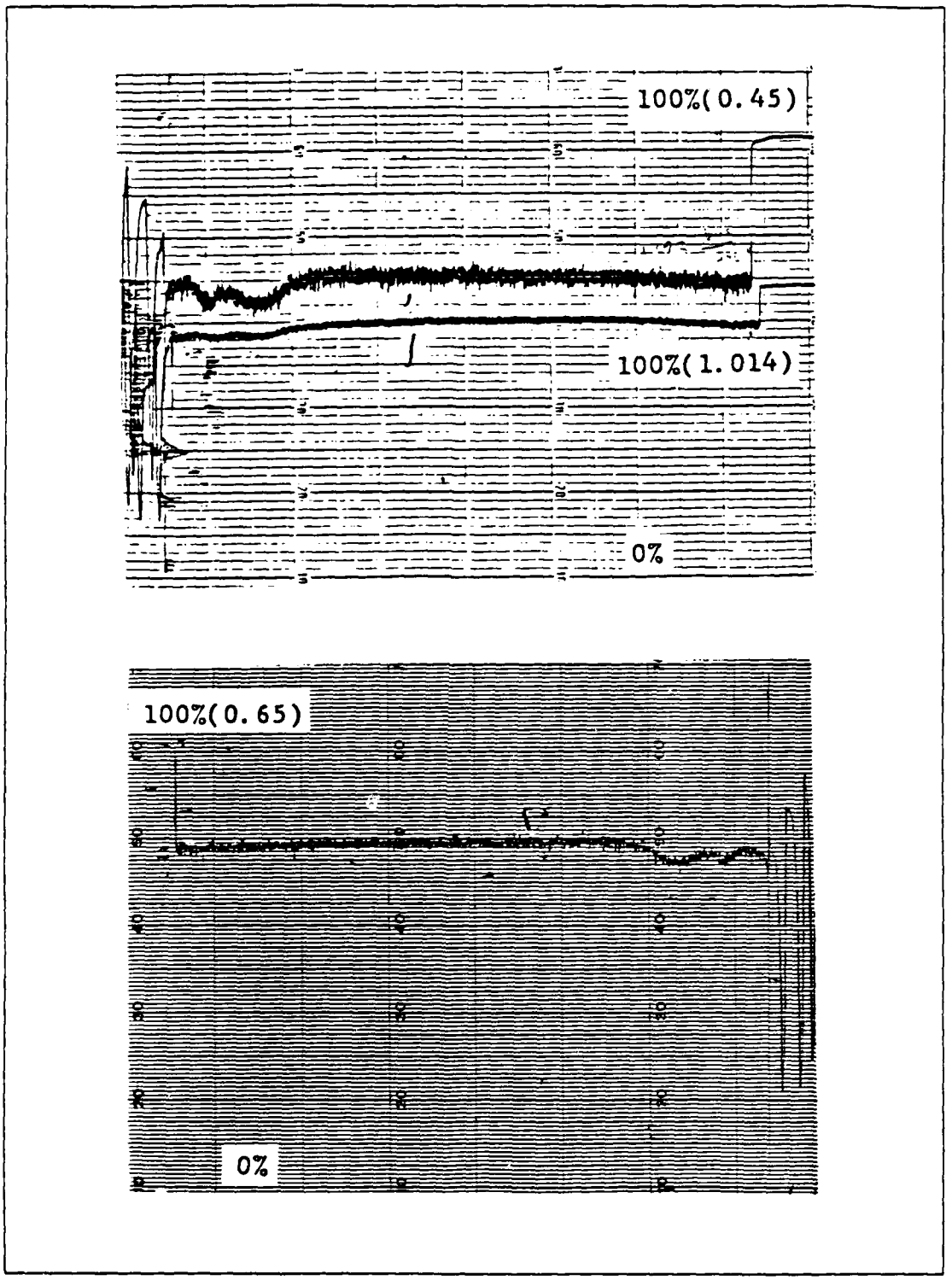

Figure 6.2 Strip Chart Recording of Run #3.

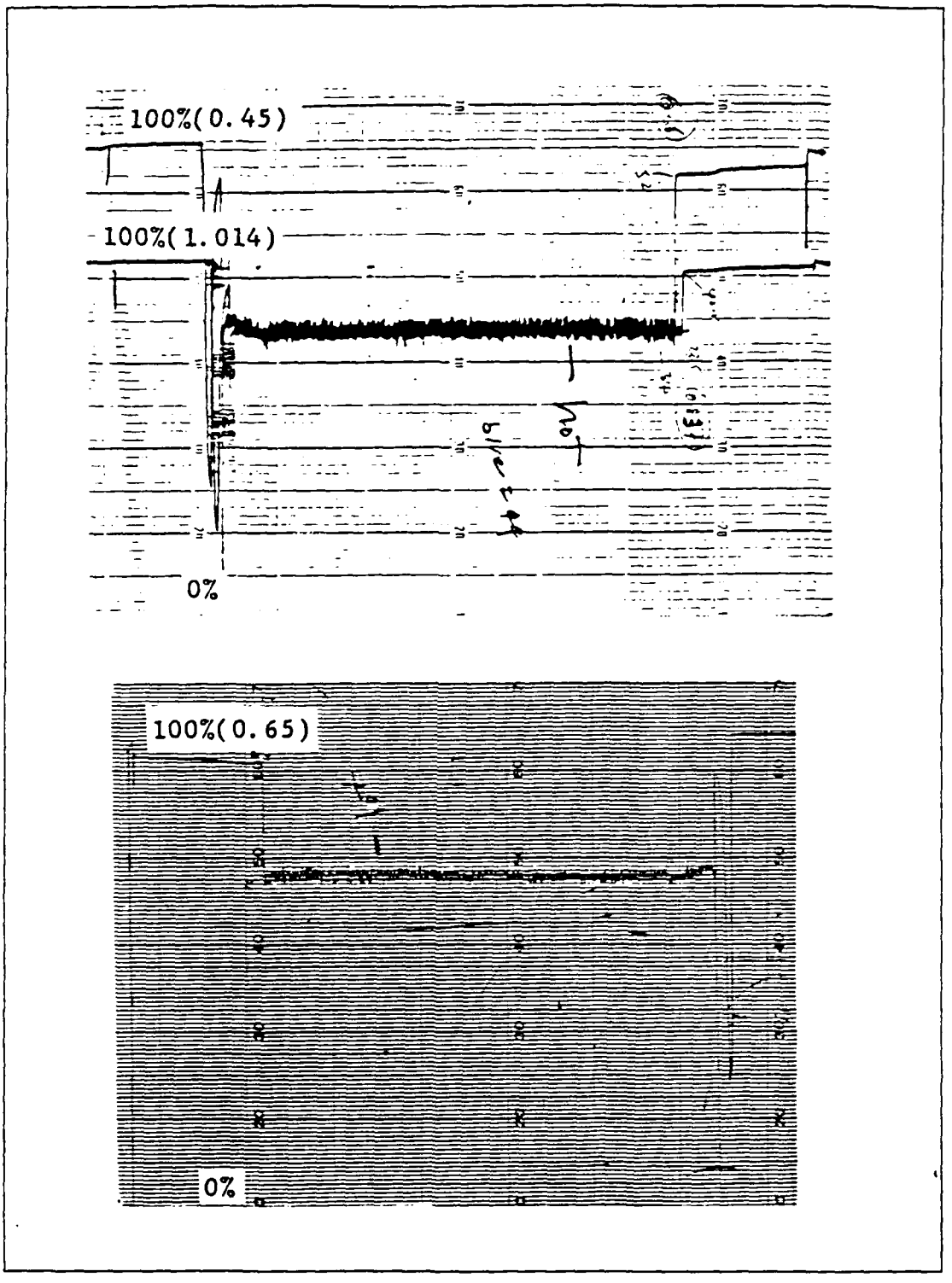

Figure 6.3 Strip Chart Recording of Run #4.

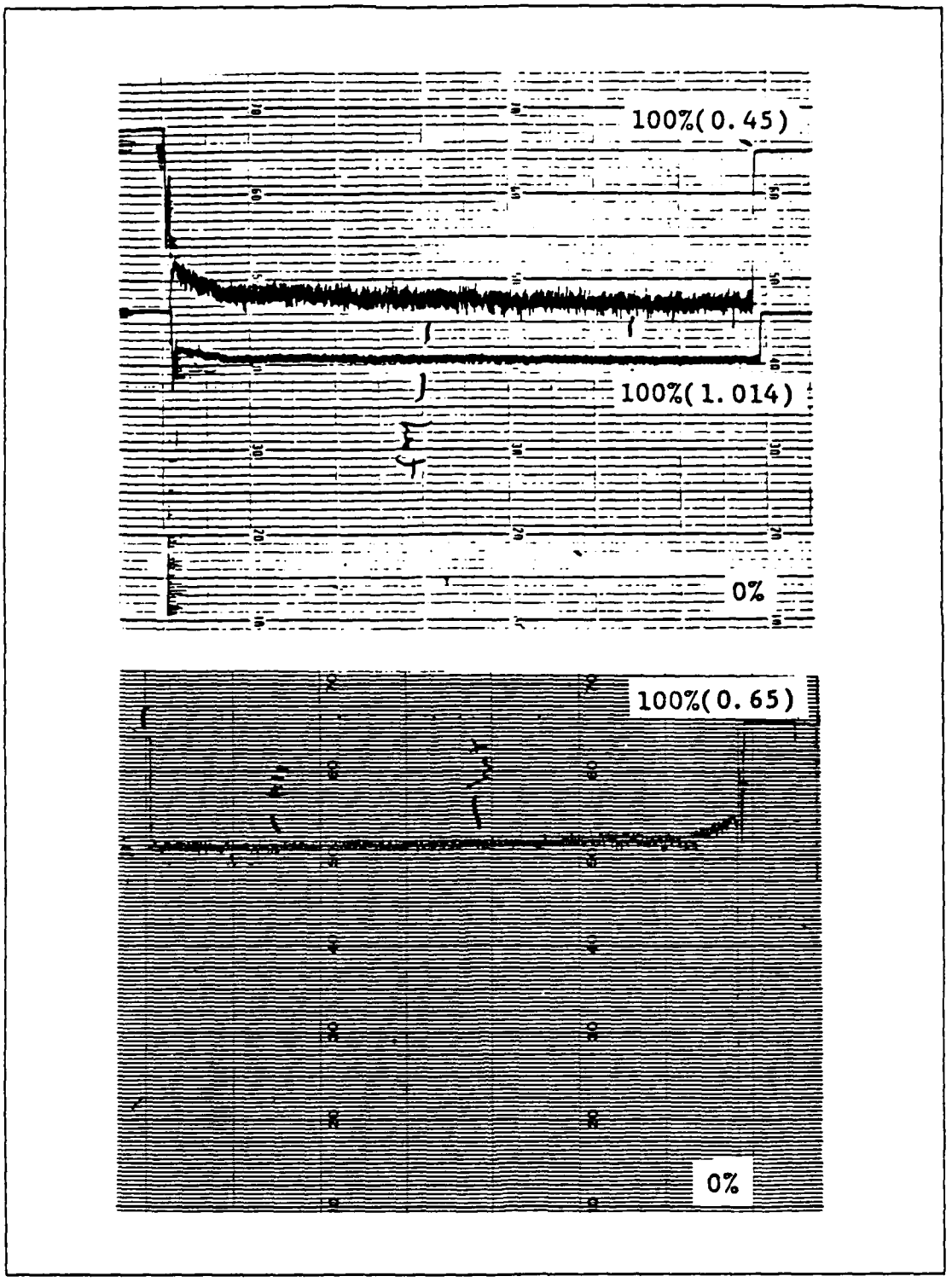

Figure 6.4 Strip Chart Recording of Run #5.

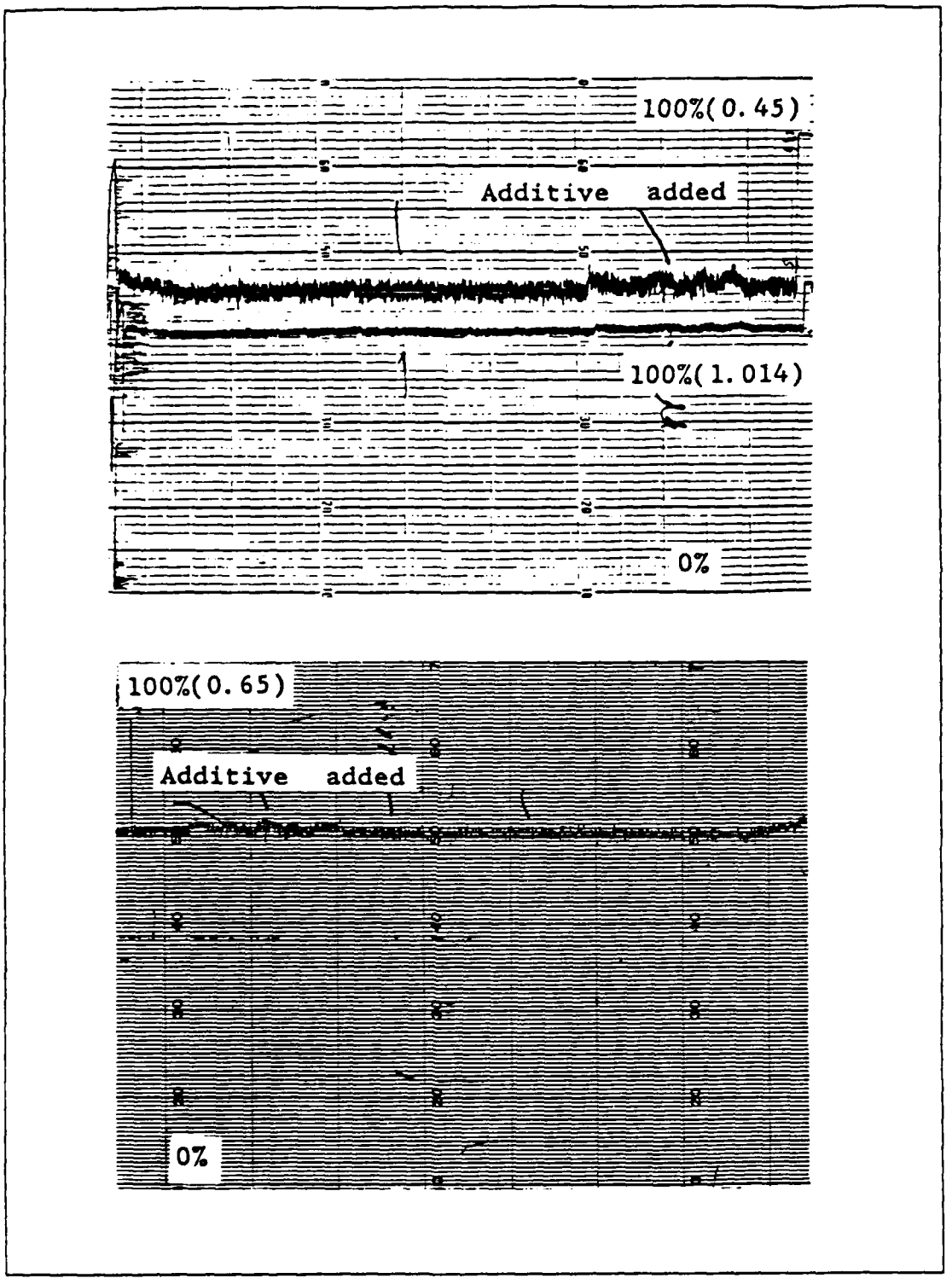

Figure 6.5 Strip Chart Recording of Run #6.

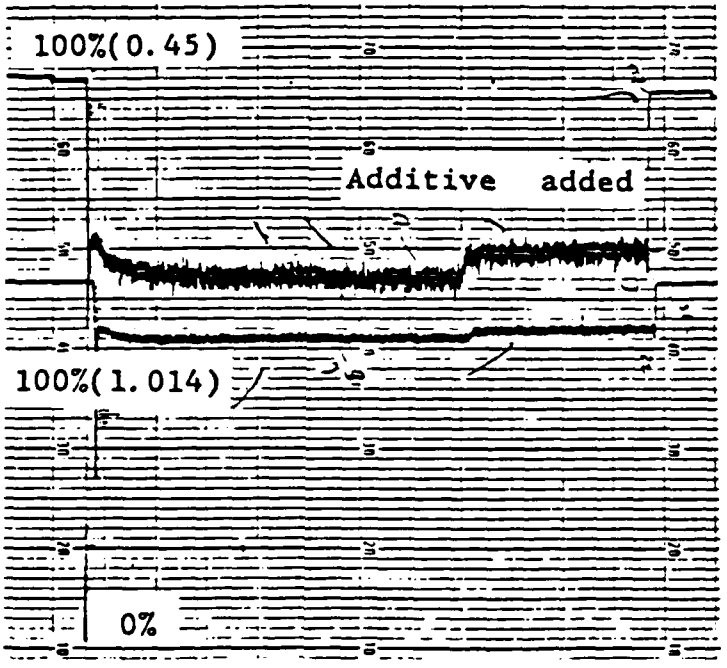

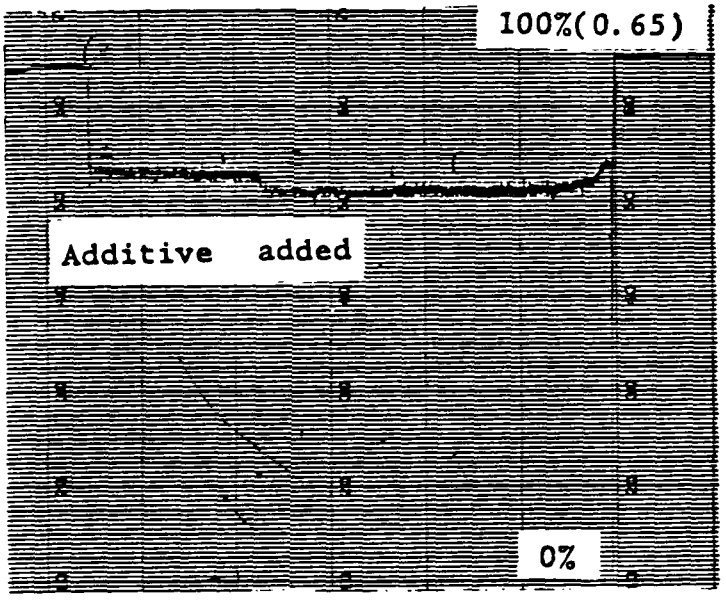

Figure 6.6 Strip Chart Recording of Run #7.

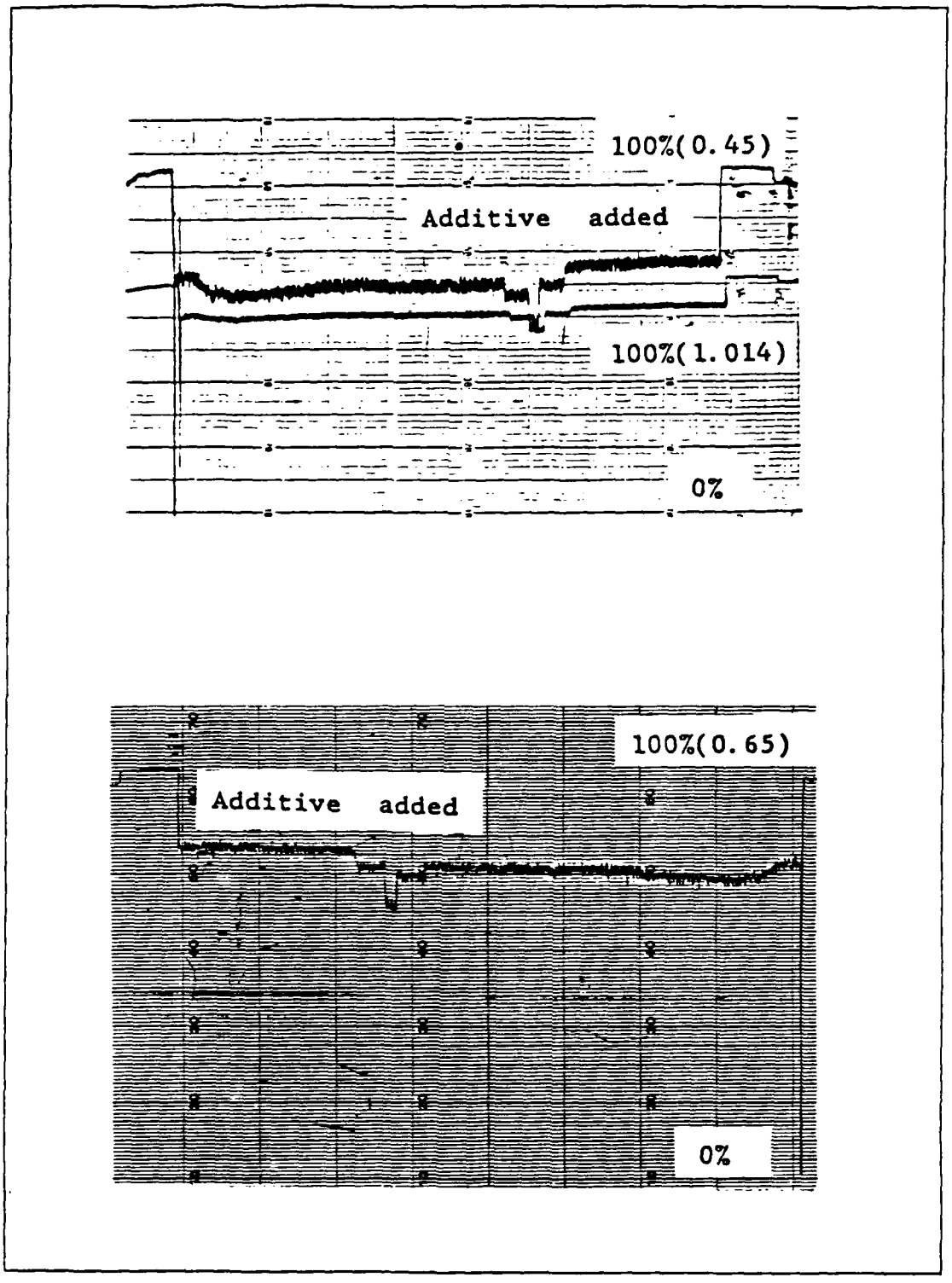

Figure 6.7 Strip Chart Recording of Run #8.

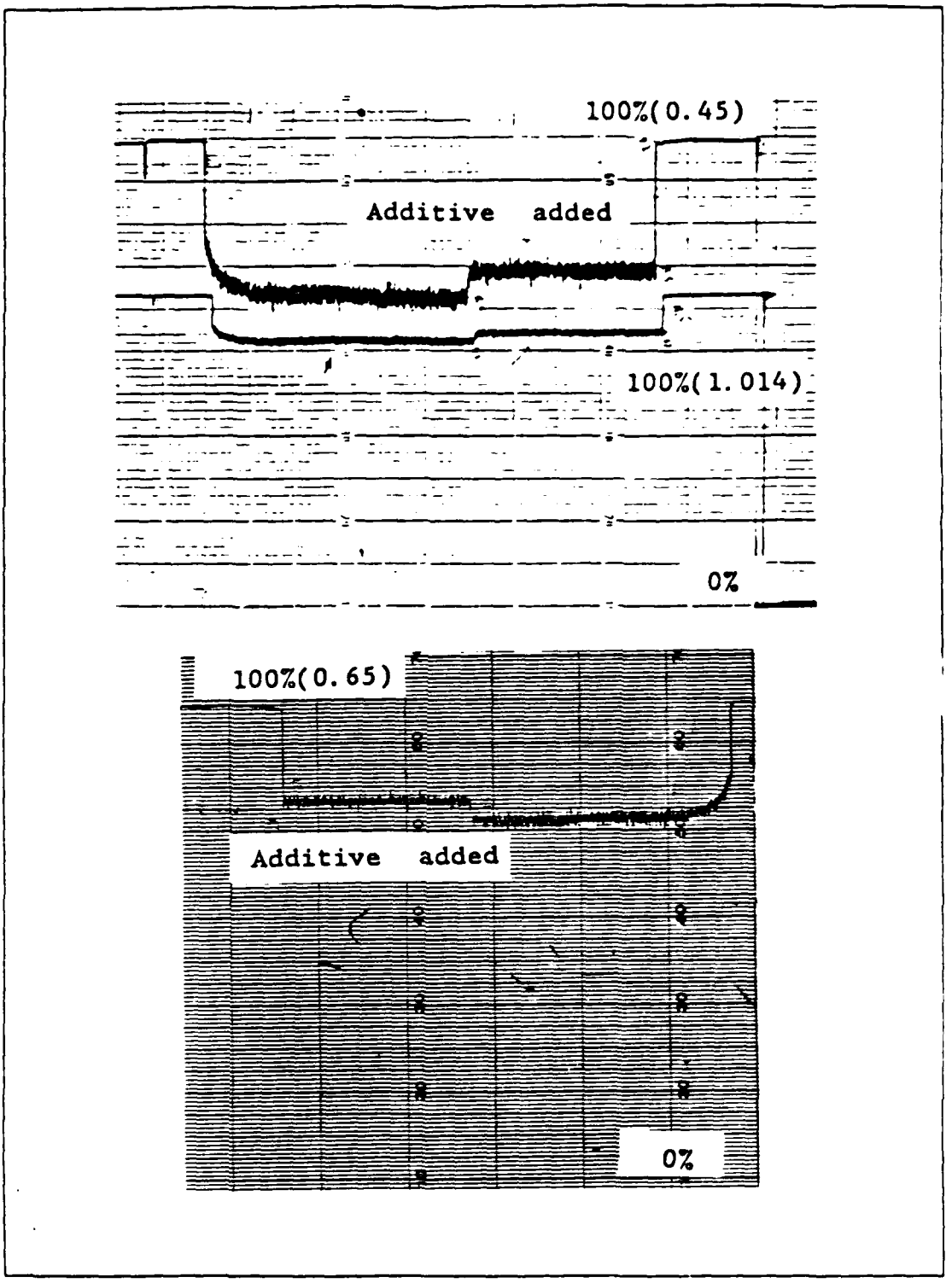

Figure 6.8 Strip Chart Recording of Run #9.

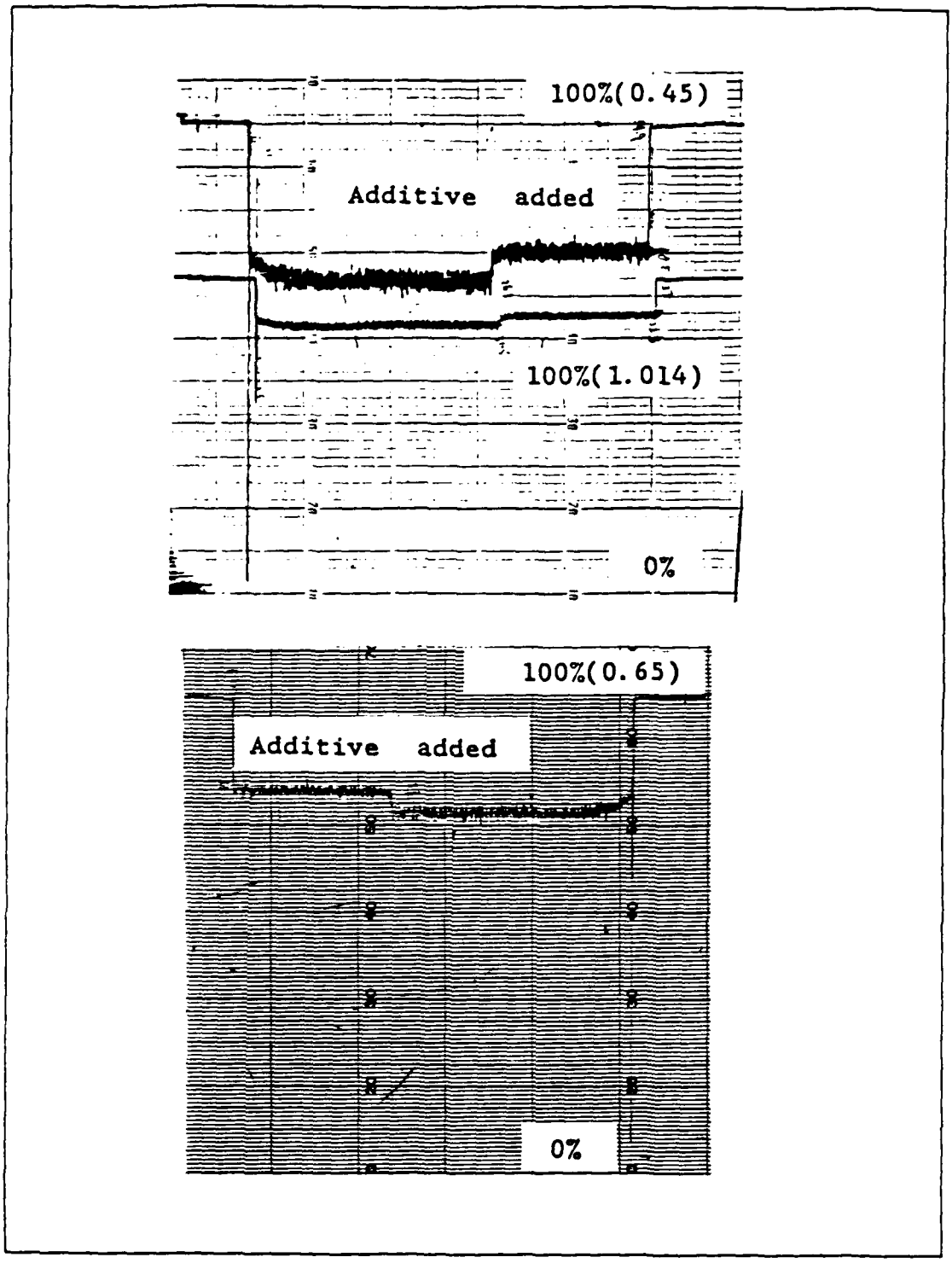

Figure 6.9 Strip Chart Recording of Run #10.

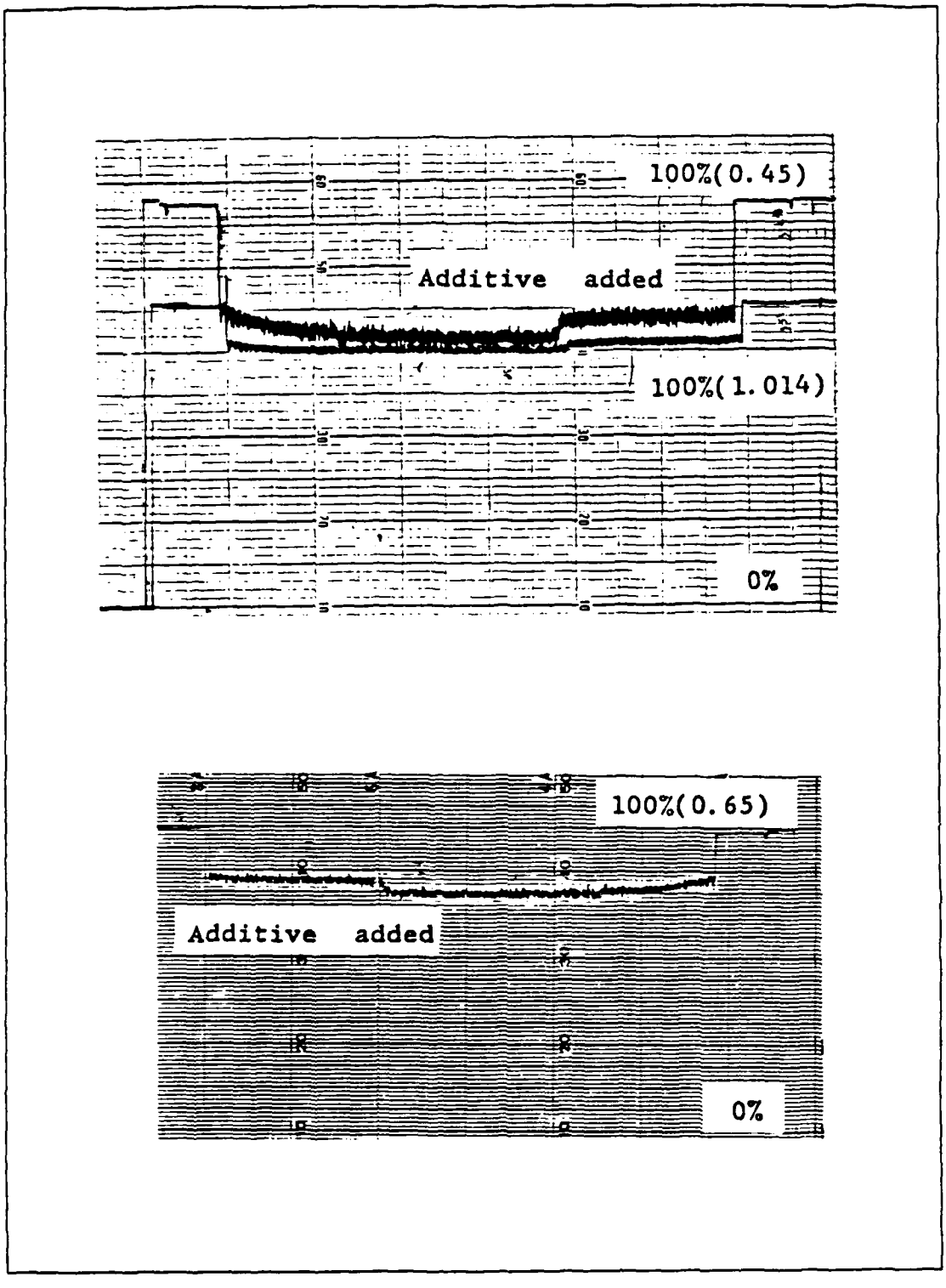

Figure 6.10 Strip Chart Recording of Run #11.

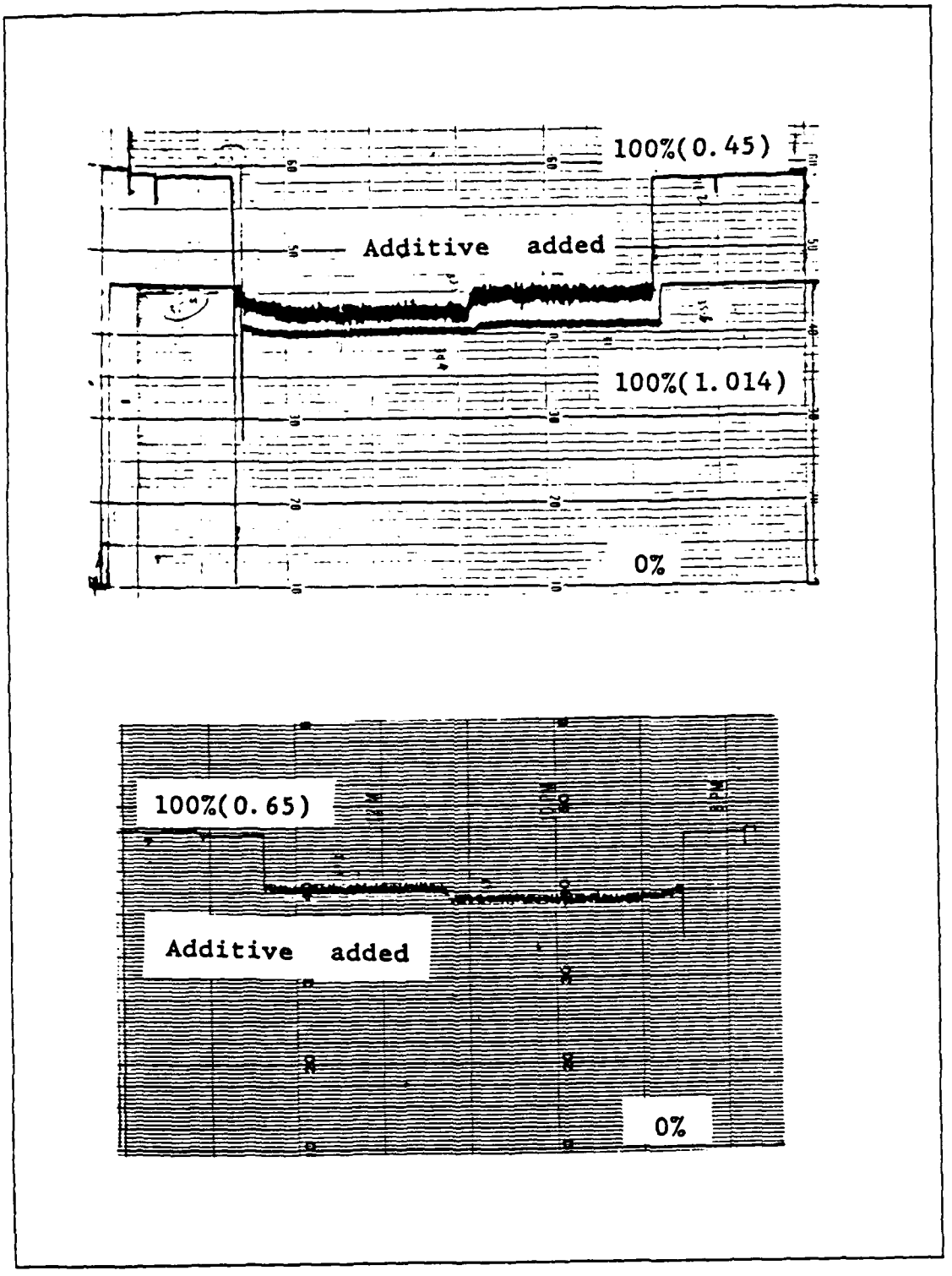

Figure 6.11 Strip Chart Recording of Run #12.

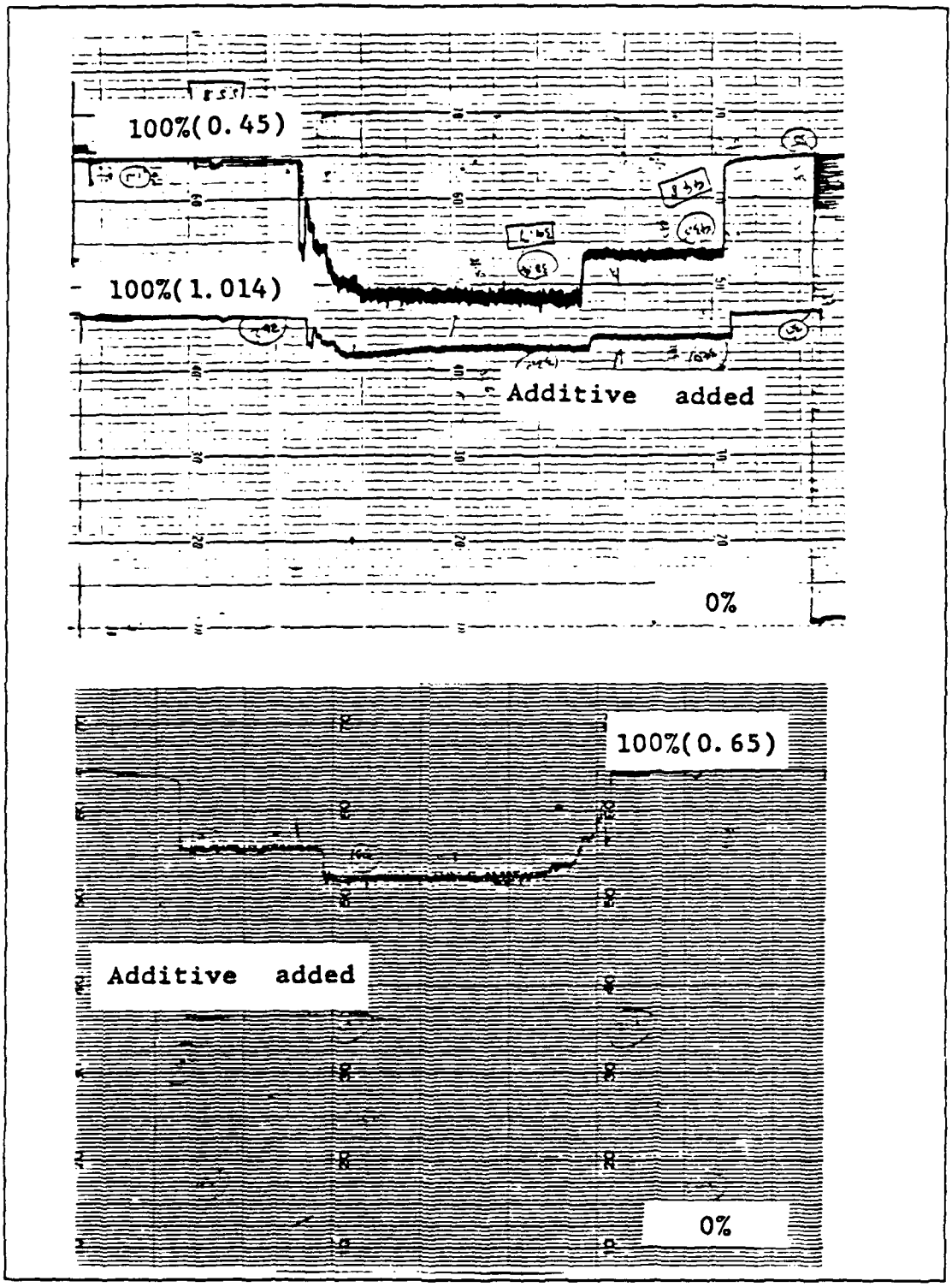

Figure 6.12 Strip Chart Recording of Run #13.

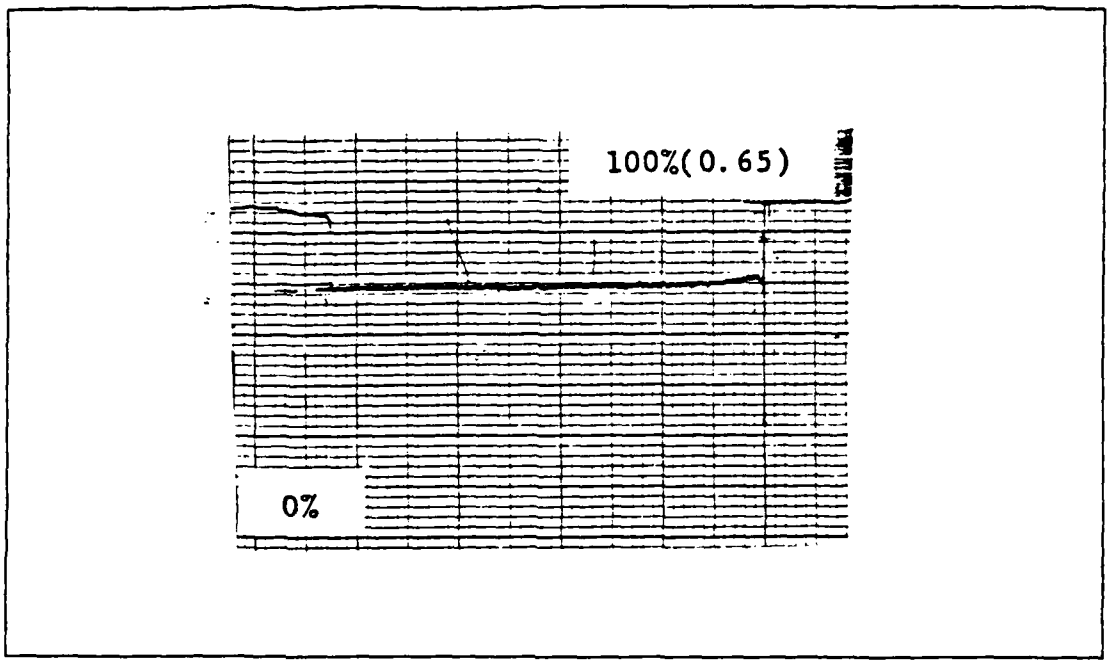

Figure 6.13 Strip Chart Recording of Run #14.

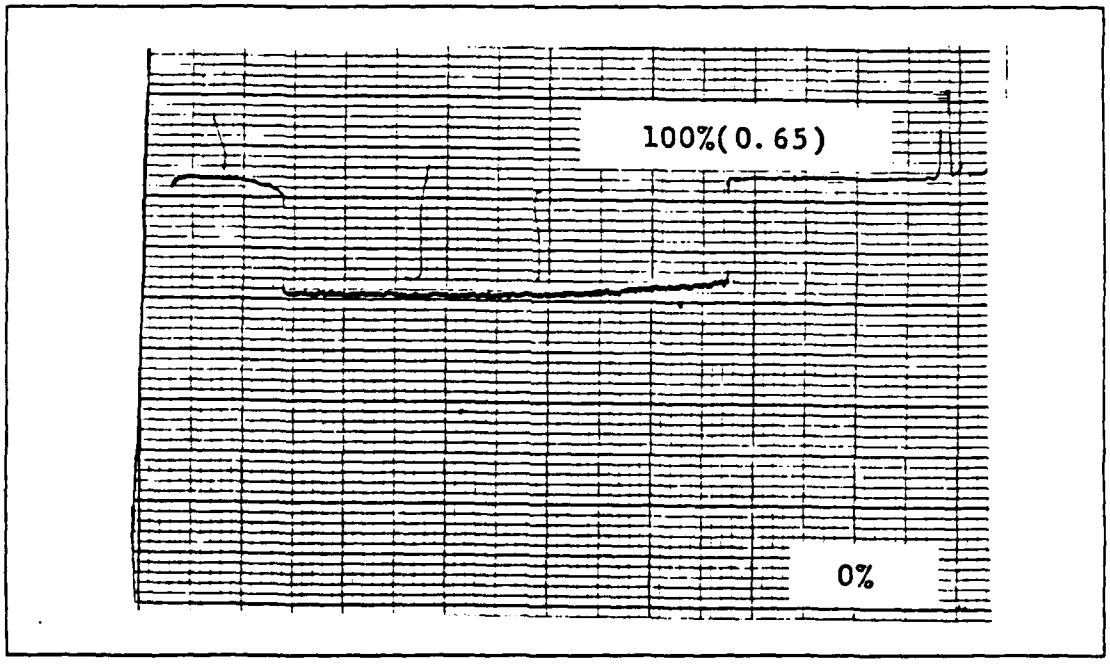

Figure 6.14 Strip Chart Recording of Run #15.

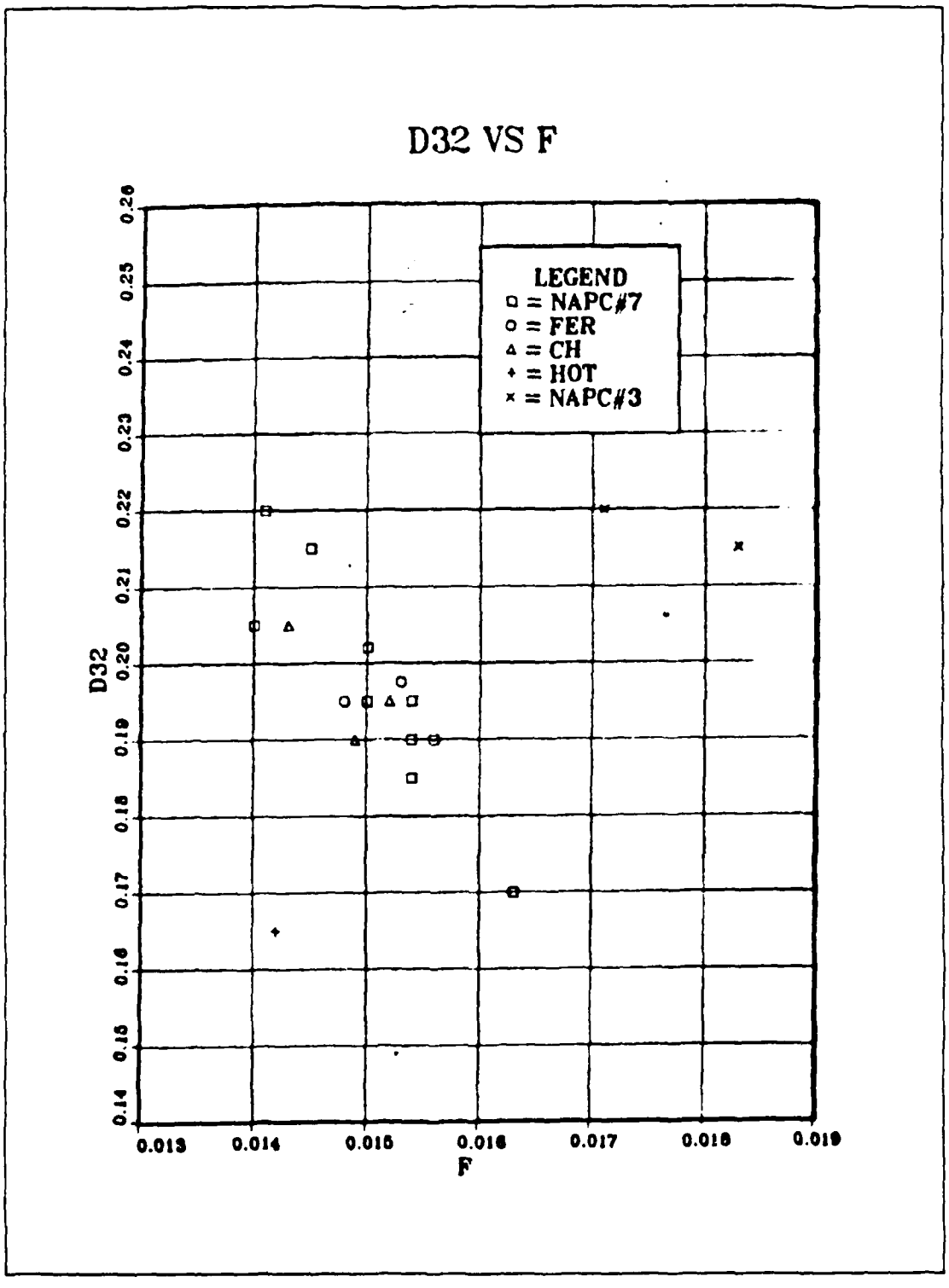

Figure 6.15 D32 vs Fuel-Air Ratio for Exhaust Region.

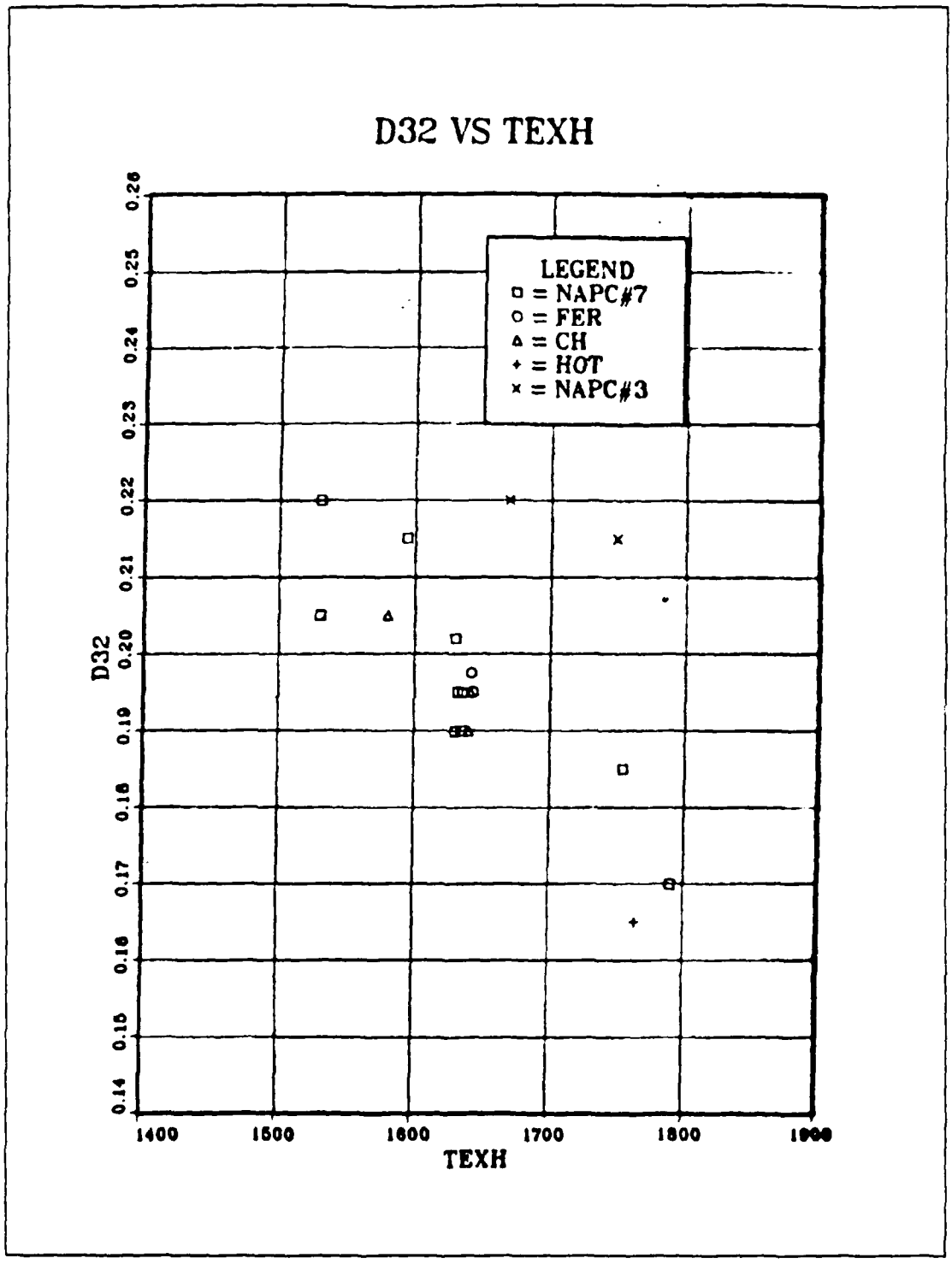

Figure 6.16 D32 vs Exhaust Temperature for Exhaust Region.

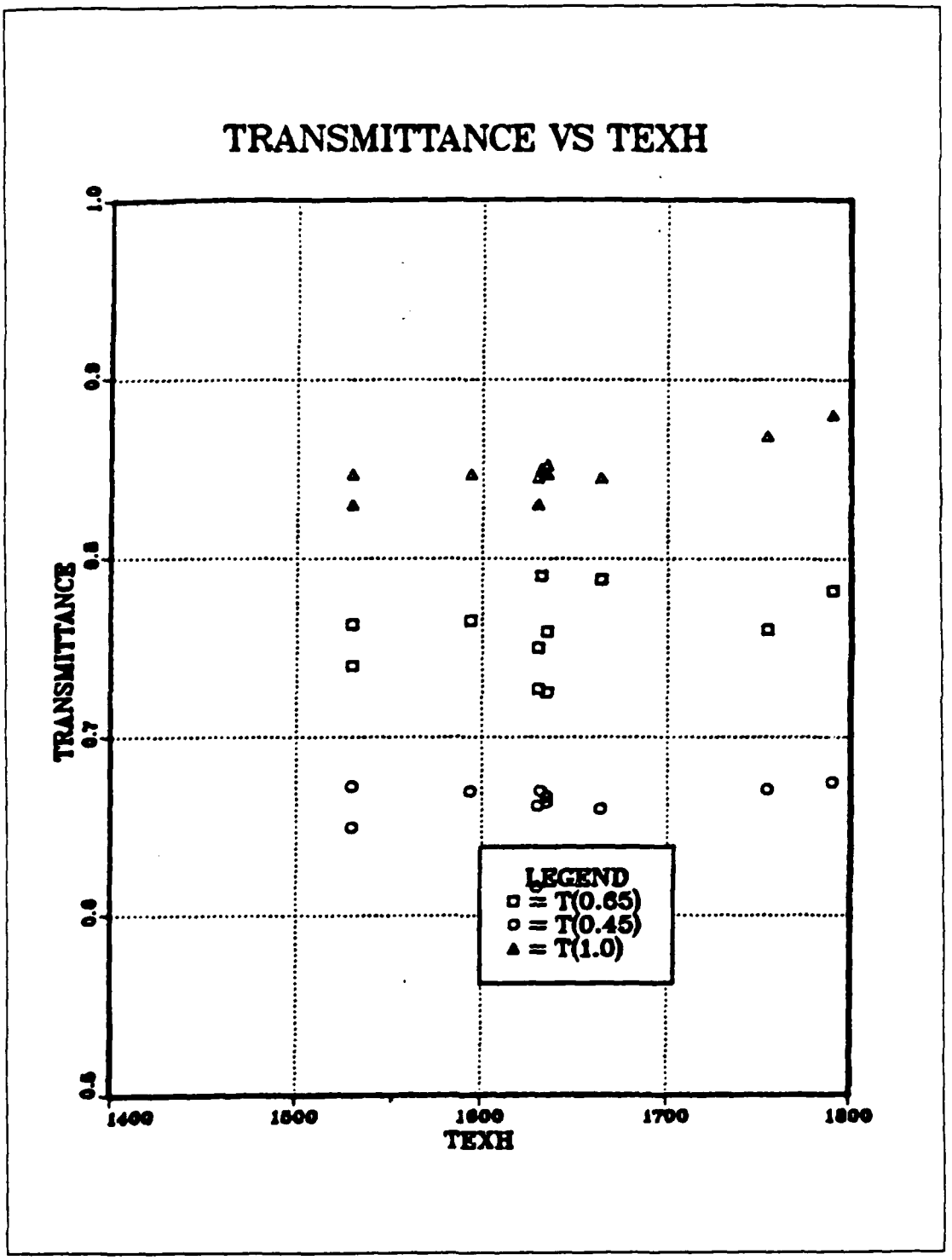

Figure 6.17 Transmittance vs Exhaust Temperature for Exhaust Region.

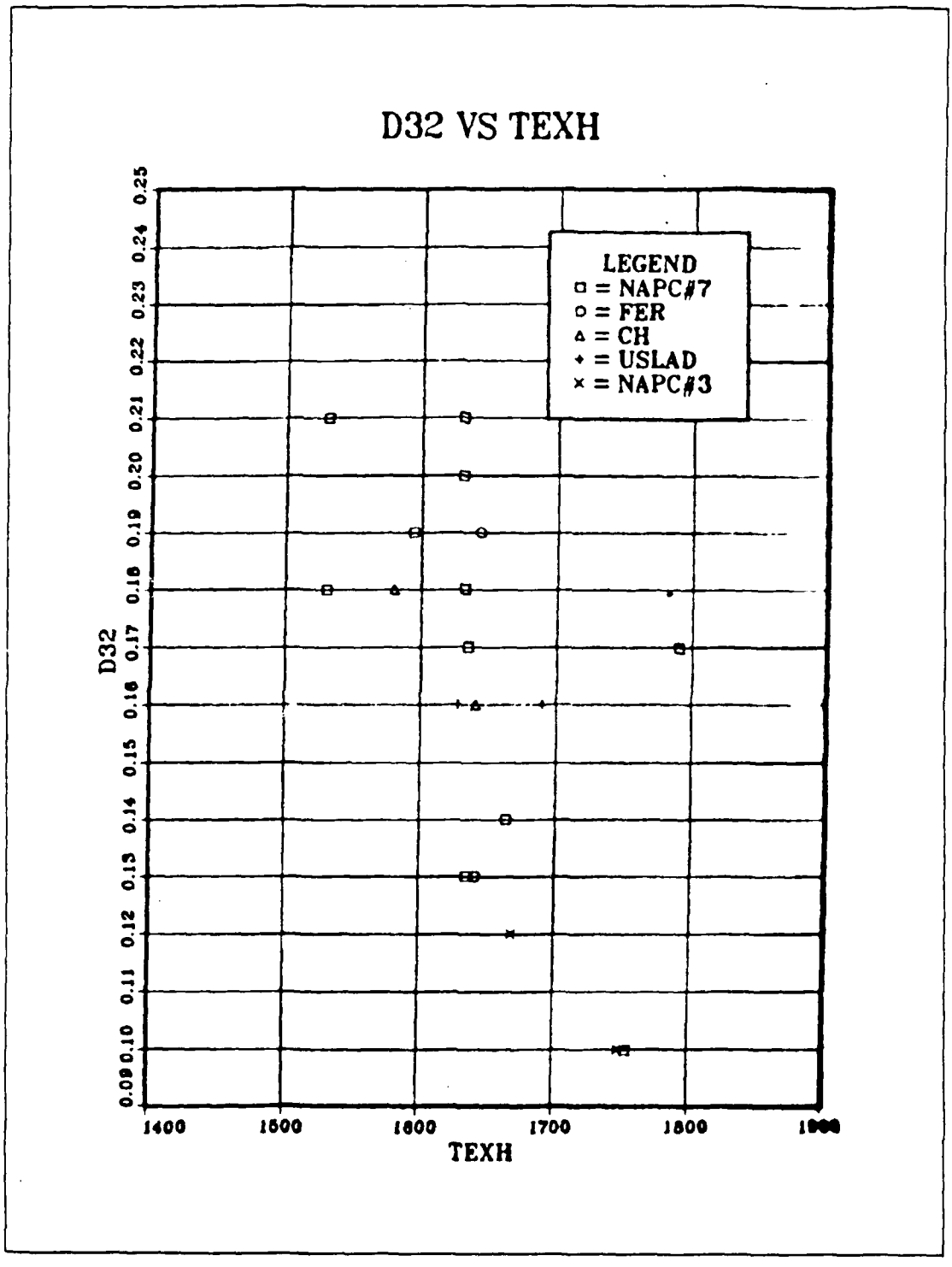

Figure 6.18 D32 vs Exhaust Temperature for Combustor Region.

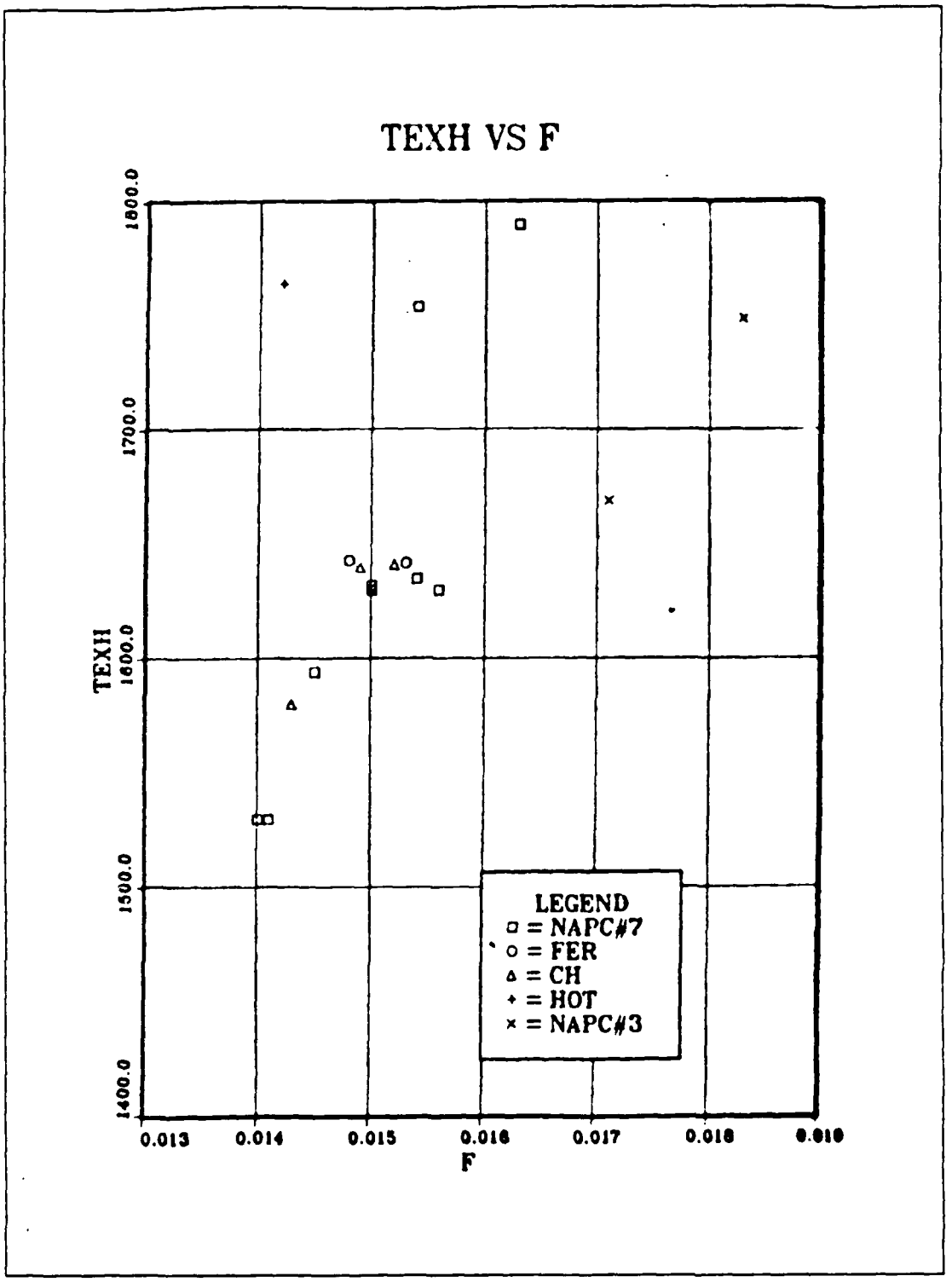

Figure 6.19 Exhaust Temperature vs Fuel-Air Ratio.

VII. CONCLUSIONS AND RECOMMENDATIONS

The results of this series of experiments indicated that Ferrocene, 12% Cerium Hex-Cem and USLAD 2055 were all effective in reducing the opacity of the exhaust gases. Particle size measurements using light transmittance methods indicated that the additives had negligible effect on mean particle diameter, indicating that the reduced opacity resulted from a reduction in soot mass concentration. However, scattered light measurements indicated that the additives resulted in a decrease in particle size. The ability to simultaneously measure scattered light and transmittance in the exhaust region during the same test should enable this discrepancy to be checked. The use of a stronger white light source, or the construction of a different set of windows for the laser beam to enter the exhaust region, would permit this to be accomplished. The use of two-wavelength transmittance measurements in the combustor region is recognised to be inadequate. The use of another wavelength in the 800nm to 1100nm range would clearly solve this problem. However, most of the lasers operating in this range have either very high power or are too large to fit conveniently into the experimental setup. Also, the inability to use scattered light measurements in the combustion region further frustrates the attempt to obtain good particle size measurements in that region. The scattered light measurements failed because there was excessive combustion light at the measurement point. One possible way to get around this problem would be to relocate the point at which the scattered light measurements are taken.

The application of optical techniques for particle size measurement to an actual gas turbine combustor introduced some practical complications. For instance, at high

temperatures, the metal combustor expands and moves. This shift in the system can upset the optical alignment of the measuring instruments, which is very critical to good measurements. In the course of this experimental work, it was found that the following procedure helped to overcome some of the problems associated with the system moving due to expansion, and improves the quality of data collected:

- The incoming light beam must be collimated and the beam diameter made smaller than the windows on the combustor can. The beam must be aligned such that it is centered on both the windows. Carrying out the above ensures that the light beam will not be disturbed by the small movements of the window tubes when the combustor is hot.
- The light beam that passes through the combustor must be aligned with the photodiode box such that a circular spot of uniform intensity is impinging on the photodiodes.
- The photodiodes give better results when the incoming light intensity (at 100% transmittance) gives an output voltage that is in the mid-range of the photodiode output. This is about 5-6 volts. If it is possible, output voltages of the photodiodes should not be below 1.0 volt (at 100% transmittance).
- Nitrogen purge rate should be set just enough to prevent soot from sticking on the windows. When the inlet air heater is operated, the nitrogen purge rate should be increased to prevent water condensation on the combustor windows.

Although all data capturing was done by the computer, at least one light transmittance output should be monitored on a strip chart recorder to allow visual observation of irregular measurements. The movement of the light beam or the combustor due to expansion can usually be detected by observing these traces. Figure 7.1 shows an irregular trace wheras Figure 7.2 shows a typical good trace.

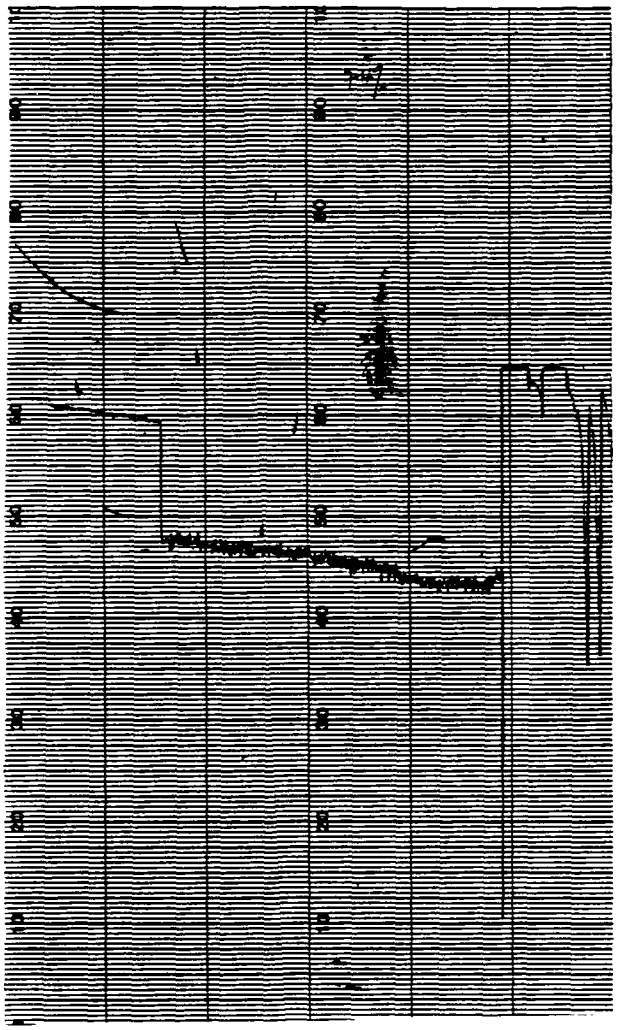

Figure 7.1 Incorrect Trace.

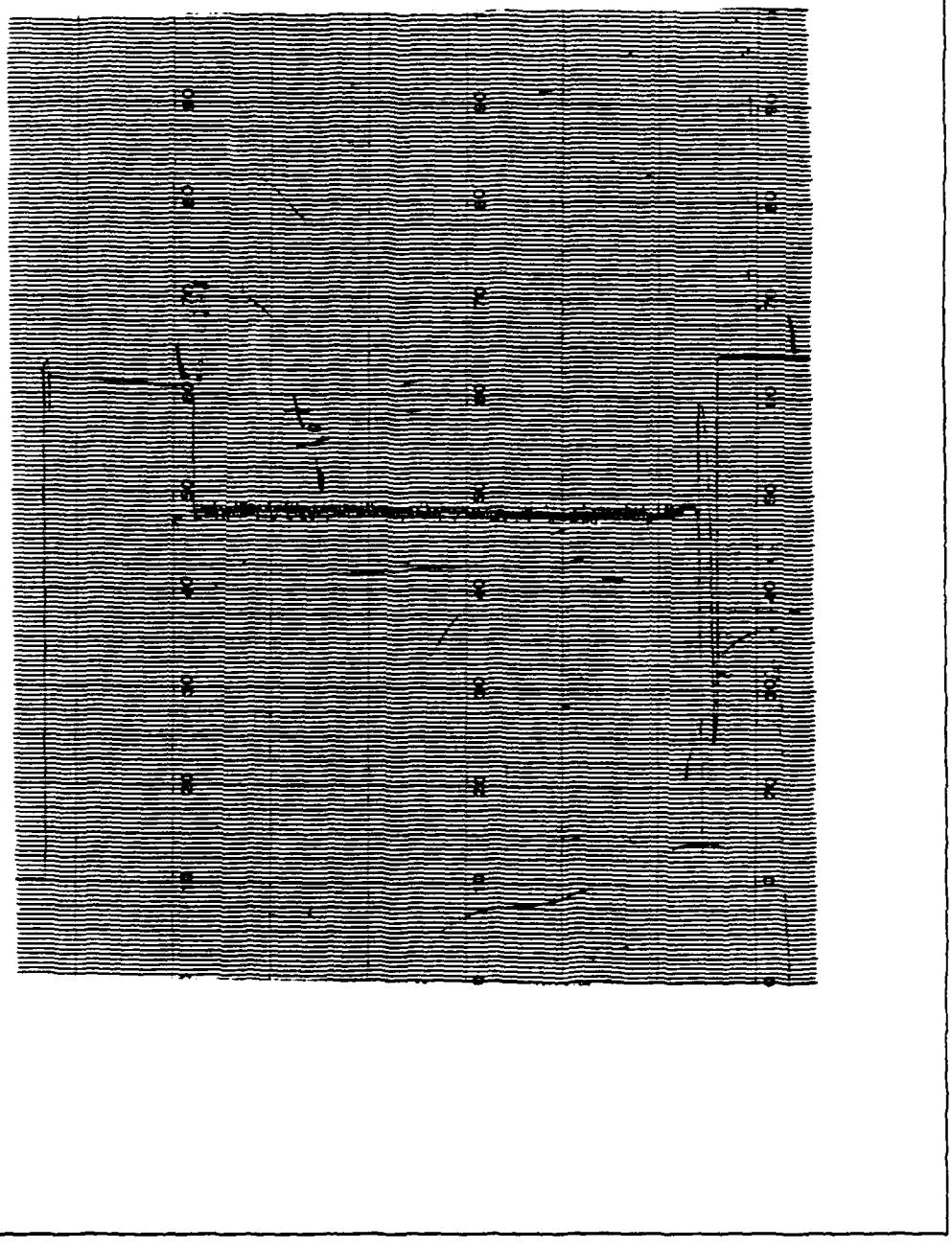

Figure 7.2 Correct Trace.

LIST OF REFERENCES

1. Bennett, J.S. *An Investigation of Particle Size Measurement Using Non-Intrusive Optical Techniques in a Gas Turnbine Combustor*, Naval Postgraduate School, CA, September, 1985

2. Cashdollar, K.L., Lee, C.K. and Singer, J.M., Three Wavelength Light Transmission Technique to Measure Smoke Particle Size and Concentration, *Applied Optics*, v.18, No. 18, pp. 1763-1769, June 1979.

3. Dobbins, R.A., and Jizmagian, G.S., Measurement of Mean Particle Size of Sprays from Diffractively Scattered Light, *AIAA Journal*, v.1,No. 8, pp. 1882-1886, August 1963.

4. Hodkinson, J.R., Particle Sizing by Means of the Forward Scattering Lobe, *Applied Optics*, v.5, No.5, pp.839-844, May 1966.

5. Powell, E.A., Cassanova,R.A., Bankston,C.P.,and Zinn,B.T., Combustion Generated Smoke Diagnostics by Means of Optical Measurement Techniques, *AIAA 14th Aerospace Sciences Meeting, Jan 1976, AIAA paper No.76-67.*

6. Naval Postgraduate School Report No. NPS67-85-004, *An Investigation of the Effects of Fuel Composition on Combustion Characteristics in a T-63 Combustor*, by D. W. Netzer and others, March 1985.

INITIAL DISTRIBUTION LIST

		No. Copies
1.	Defense Technical Information Center Cameron Station Alexandria, Virginina 22304-6145	2
2.	Library,Code 0142 Naval Postgraduate School Monterey, California 93943-5002	2
3.	Department Chairman, Code 67 Department of Aeronautics Naval Postgraduate School Monterey, California 93943-5000	1
4.	Professor D. W. Netzer, Code 67Nt Department of Aeronautics Naval Postgraduate School Monterey, California 93943-5000	2
5.	CPT Jway Ching Hua Block 29 Outram Park #12-495 S 0316 Republic of Singapore	2

END

DTIC

11-86